


Research Article

Glaciations and landscape change in the Lower Aare Valley (Northern Switzerland) through the Middle Pleistocene

Lukas Gegg^{a,b} , Flavio S. Anselmetti^b, Gaudenz Deplazes^c, Alexander Fuelling^a, Herfried Madritsch^{c,d}, Daniela Mueller^{a,e}, Frank Preusser^a, and Marius W. Buechi^b

^aInstitute of Earth and Environmental Sciences, University of Freiburg, Albertstraße 23b, 79104 Freiburg, Germany; ^bInstitute of Geological Sciences and Oeschger Centre for Climate Change Research, University of Bern, Baltzerstrasse 1+3, 3012 Bern, Switzerland; ^cNational Cooperative for the Disposal of Radioactive Waste (Nagra), Hardstrasse 73, 5430 Wettingen, Switzerland; ^dPresent address: Federal Office of Topography swisstopo, Seftigenstrasse 264, 3084 Wabern, Switzerland and ^ePresent address: Department of Geography and Planning, School of Environmental Sciences, University of Liverpool, Liverpool L69 3BX, United Kingdom

Abstract

Throughout the Pleistocene, valley glaciers repeatedly advanced into the forelands of the European Alps. However, the corresponding geological record is highly fragmentary and the regional glaciation history, especially prior to the last glacial maximum, is still poorly documented. We explored the archives of the Lower Aare Valley in the confluence area of the Aare river with Reuss and Limmat, focusing on the overdeepened Gebenstorf-Stilli Trough. In four scientific boreholes, ~350 m of drill cores were recovered, and complemented with investigations of outcrops and reflection seismics in the nearby glaciofluvial Habsburg-Rinikerfeld Palaeochannel. The integrative interpretation of these data provides new insights into the local landscape evolution: We identified two generations of glacial basin infill in the Gebenstorf-Stilli Trough that are overlain by glaciofluvial gravels, and two distinct glaciofluvial gravel bodies in the neighboring paleochannel. In this specific local setting, gravel petrographic compositions and their statistical analysis prove to be powerful tools to identify inputs from the confluent catchments, to aid in lithostratigraphic classification, and to interpret the depositional and landscape histories. We suggest that it is mainly the penultimate glaciation, characterized by three separate ice advances, that shaped the present-day study area, and whose deposits are preserved in the Middle Pleistocene archives.

Keywords: Glacial basin; glaciation history; glaciofluvial gravel; Hochterrasse; overdeepening; penultimate glaciation; scientific drilling

Introduction

During the Pleistocene, Alpine glaciers repeatedly advanced into the mountain foreland, temporarily covering large parts of Northern Switzerland and neighboring regions (Fig. 1; Preusser et al., 2011). These glaciations had a significant geomorphic effect on their surroundings through glaciofluvial dissection and subglacial erosion of overdeepened basins, but also through accumulation of decameter-thick clastic deposits. The alternating phases of erosion and deposition (cf., Buechi et al., 2018) cause a major difficulty hindering Quaternary research in alpine environments, because the result is a fragmentary and incomplete geological record. This way, the remnants of entire glaciations may have been eroded and entirely obliterated by later ice advances (Hughes et al., 2019; Merritt et al., 2019). Thus, the glacial stratigraphy and landscape history prior to the last glaciation remains intricate and poorly constrained not only in Northern Switzerland but in mountainous or polar terrestrial settings worldwide.

Previous studies have suggested the occurrence of up to 15 extensive glaciations of the Swiss Alps throughout the Pleistocene, but only five major phases of ice advance into the foreland could be pinpointed and their extents roughly mapped (Preusser et al., 2011; Graf and Burkhalter, 2016; Schlüchter et al., 2021). Four of them are attributed to the Middle Pleistocene, and are termed, from oldest to youngest, Möhlin, Habsburg, Hagenholz, and Beringen (Fig. 1; Graf, 2009a; Preusser et al., 2011). While the Beringen Glacial has been correlated with reasonable confidence with marine oxygen isotope stage (MIS) 6 (ca. 150 ka; MIS after Lisiecki and Raymo, 2005; Dehnert et al., 2012; Lowick et al., 2015), the chronostratigraphic positions of older glaciations are poorly constrained. It is also not entirely clear whether all of them represent separate full glaciations, or individual advances within a particular glaciation (cf., the threefold Late Pleistocene Birrfeld Glacial, Fig. 1; Preusser, 2004; Ivy-Ochs et al., 2008; Seguinot et al., 2018). Based on presumed correlative gravel deposits in the downstream-adjacent Upper Rhine Graben (Fig. 1), Preusser et al. (2021) suggested a correlation of Habsburg with MIS 8 or 10 (ca. 270 ka or ca. 340 ka), and of Möhlin (the ‘most extensive glaciation’) with MIS 12 (ca. 420 ka; see also Dieleman et al., 2022b). Subdivision of the respective deposits was done through extensive and detailed fieldwork and further analyses (e.g., gravel petrographic and heavy mineral analysis) but gave rise to a patchwork of local morpho-

Corresponding author: Lukas Gegg; Email: lukas.egg@geologie.uni-freiburg.de

Cite this article: Gegg, L., Anselmetti, F.S., Deplazes, G., Fuelling, A., Madritsch, H., Mueller, D., Preusser, F., Buechi, M.W., 2025. Glaciations and landscape change in the Lower Aare Valley (Northern Switzerland) through the Middle Pleistocene. *Quaternary Research* 125, 134–153. <https://doi.org/10.1017/qua.2024.61>



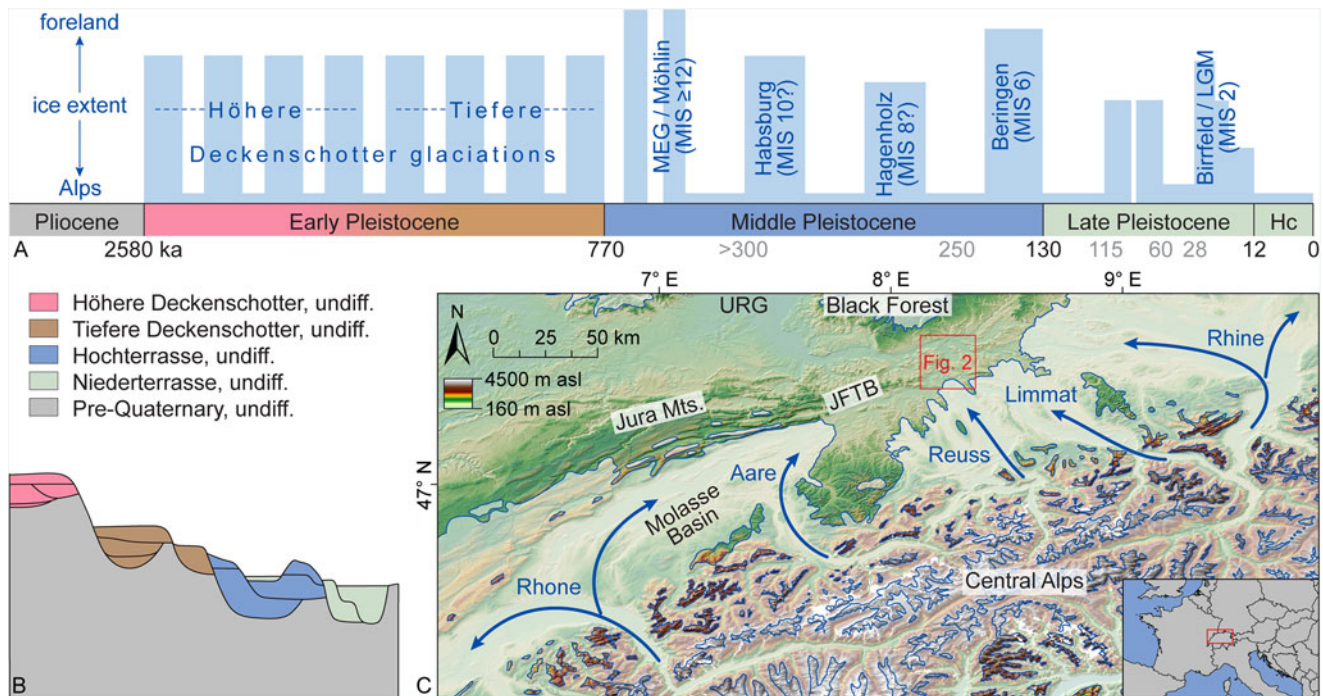


Figure 1. Quaternary glaciation history and related deposits in Northern Switzerland. (A) Sketch of timing and extent of ice advances (modified after Preusser et al., 2011; Schlüchter et al., 2021); MEG = most extensive glaciation, LGM = last glacial maximum, Hc = Holocene. (B) The corresponding, composite lithostratigraphic units, mainly glaciofluvial gravels, occur at different elevation levels (modified after Graf and Burkhalter, 2016). (C) Location of the study area (red box labeled 'Figure 2') in central Northern Switzerland (background: SRTM DEM, van Zyl, 2001; JFTB = Jura fold-and-thrust-belt; URG = Upper Rhine Graben). The ice extent during the LGM (from Ehlers et al., 2011) is shaded white, and the main piedmont glacier lobes are labeled.

and lithostratigraphic schemes that are not always straightforward to correlate (Graf, 2009a).

Because geological archives are scarce, such uncertainties are not trivial to resolve. Promising approaches are the exploration of sedimentary records of previous lakes, often hosted in subglacial overdeepenings, that contain the most complete and best-resolved Quaternary successions in the region (e.g., Schlüchter, 1989; Nitsche et al., 2001; Preusser et al., 2005; Dehnert et al., 2012; Buechi et al., 2018, 2024; Schwenk et al., 2022a, 2022b; Gegg et al., 2023; Schaller et al., 2023; Schuster et al., 2024), and of abandoned sandurs where glaciofluvial material was spared from erosion (e.g., Graf, 2009a; Claude et al., 2017; Dieleman et al., 2022b; Pfander et al., 2022). In the present study, we combined these two approaches, and present results from scientific drillings from an overdeepened trough, and from both drilling and outcrop investigations in a nearby paleochannel. Based on sedimentological analyses complemented by reflection seismics, we aim to reconstruct and refine the local- to regional-scale glaciation and landscape history, specifically throughout the Middle Pleistocene.

Study area and stratigraphy

The confluence area of the Aare, Reuss, and Limmat rivers in Northern Switzerland, frequently referred to as 'Wasserschloss', is a key site for the Quaternary geology of the northern Alpine foreland (Fig. 2; Dick et al., 1996). The 'Wasserschloss' is located about 50 km northwest of the Alpine front, at the eastern margin of the Jura Mountains (Fig. 1). The latter consist of Mesozoic sedimentary rocks (carbonates, marls, and siliciclastics) deposited in an epicontinental sea (Bitterli et al., 2000; Bitterli-Dreher et al.,

2007; Jordan et al., 2008). In the early Paleogene, this sedimentary succession was uplifted on the forebulge of the approaching Alpine orogeny, while to the south of it, the Molasse Basin subsided (Pfiffner, 1986; Burkhard and Sommaruga, 1998; Berger et al., 2005). The deposition of heterogeneous Molasse sands, silts, and marls progressed northward, reached the southern part of the study area in the Oligocene, but stopped in the Late Miocene with the development of the Jura fold-and-thrust belt (JFTB; Burkhard, 1990; Looser et al., 2021; Madritsch et al., 2024). In the JFTB, the Mesozoic strata are folded and often steeply dipping, while they are little deformed and sub-horizontal farther north. The lithologically and structurally complex bedrock architecture gave rise to the study area's varied topography, which is different from many other Quaternary sites of the Alpine foreland (Fig. 2; Ziegler and Fraefel, 2009; Yanites et al., 2017; Gegg et al., 2021).

Regionally, the Quaternary was not only characterized by a trend of cooling climate and extensive ice advances, but also by repeated lowering of the fluvial base level (Schlunegger and Mosar, 2011; Kuhlemann and Rahn, 2013; Yanites et al., 2017). Remnants of two gravel units occurring at hill tops are referred to as 'Höhere Deckenschotter' (found at ~520–600 m asl in the study area) and 'Tiefere Deckenschotter' (~450–520 m asl), respectively, and represent the Early Pleistocene (Fig. 1; Akçar et al., 2017; Dieleman et al., 2022a; Thew et al., 2024). Intercalated diamicts interpreted as tills suggest that the corresponding paleoglaciers already reached far into the foreland (Graf, 1993, 2009b). Along with a major base level drop, the Deckenschotter river valleys were abandoned, and a new drainage network established (Graf, 2009a, b). In the Wasserschloss area, it consists of the Habsburg-Rinikerfeld Palaeochannel (HRPC; Fig. 2) and its northward continuation via the Ruckfeld area into the High Rhine Valley. Through

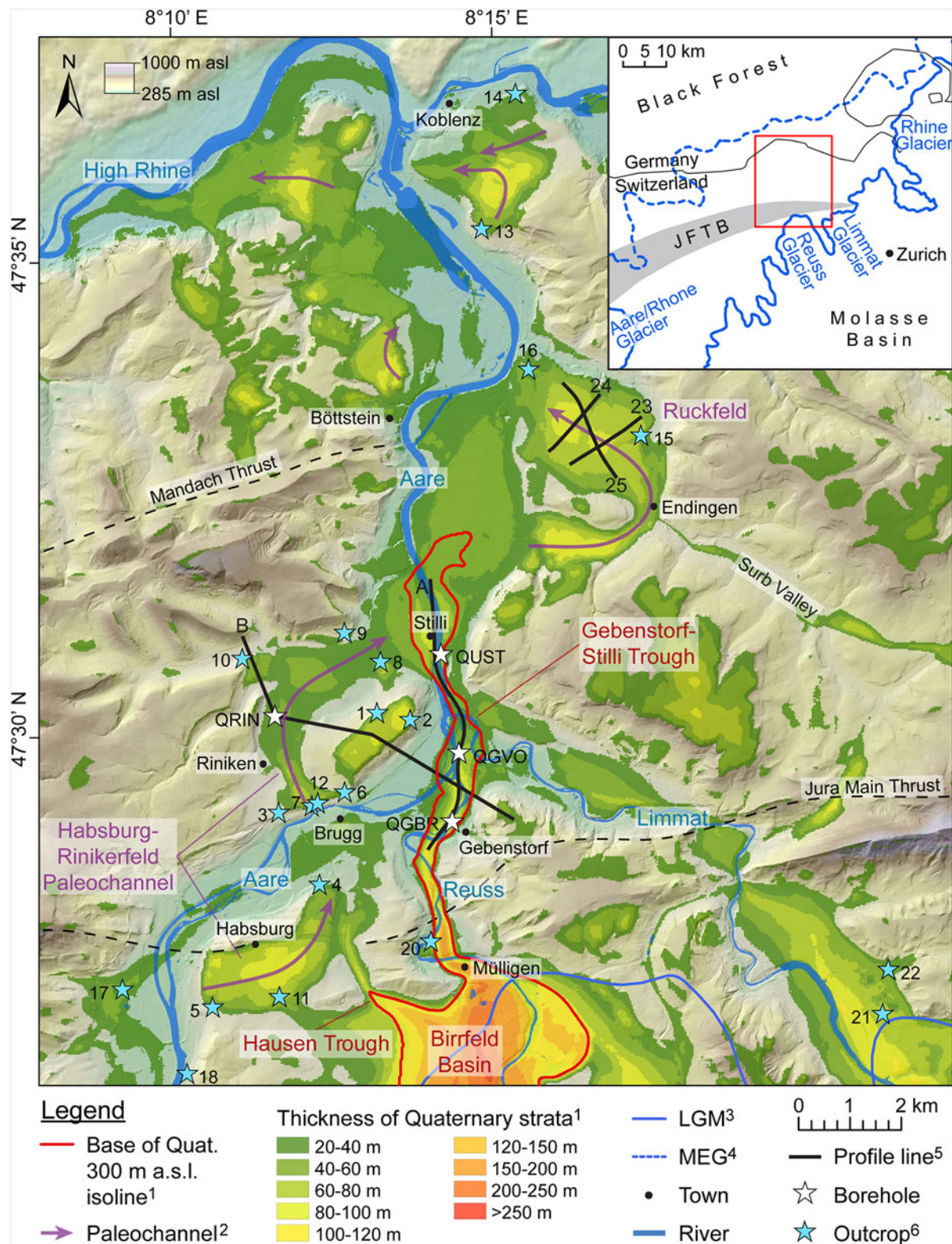


Figure 2. Overview map of the Wasserschloss area in Northern Switzerland (background: LiDAR DEM; Swisstopo, 2011). Inset shows the major geological units around the study area as well as the relevant paleoglaciers lobes (see Figure 1). Legend notes: ¹from Pietsch and Jordan (2014), Gegg et al. (2021), and references therein; ²after Graf (2009a); ³alpine ice extent of the last glacial maximum (Bini et al., 2009); ⁴ice extent of the most extensive glaciation (Keller and Krayss, 2010); ⁵A and B refer to constructed sections (Figures 10 and 11, respectively); 23, 24, and 25 are seismic lines (Figure 9); ⁶outcrop numbers refer to Supplementary Table 2. Outcrops mentioned in the text: 5 (Götschel), 6 (Hansfluhsteig), 9 (Haselloch), 10 (Alpberg), 13 (Hönger). Note: outcrop 19 lies slightly south of the map extent.

this pathway, glaciofluvial drainage as well as glacial advances occurred repeatedly throughout most of the Middle Pleistocene (Graf, 2009a; Gegg et al., 2023).

The main remnants of the Middle Pleistocene glaciations are glaciofluvial sediments referred to as Hochterrasse (high terrace) based on their position well above the modern valley bottom. An internal lithostratigraphic subdivision of the Hochterrasse has been achieved based on gravel petrographic and heavy mineral compositions, which show that gravel units of different provenance occur at similar elevations (Fig. 1; ~350–420 m asl). In our study area, the Hochterrasse is thus subdivided into three units (Habsburg Gravel, Ruckfeld Gravel, and Remigen Gravel) which are named after their type locations (Bitterli-Dreher et al., 2007; Graf, 2009a). These gravel units presumably represent three out of the four regionally identified Middle Pleistocene glaciations (Habsburg, Hagenholz, Beringen), and are correlated with the morphostratigraphically defined Upper, Middle, and Lower Hochterrasse, respectively, of the Lower Aare Valley farther downstream (Matousek et al., 2000). Occasional intercalated tills and glaciotectionic deformation in the Remigen Gravel and basal diamicts in the HRPC suggest that at least two of the Middle Pleistocene ice advances reached into the study area (Graf, 2009a; Gegg et al., 2023).

The Middle Pleistocene presumably also marked the onset of overdeepening in the midlands of Northern Switzerland (i.e., the subglacial carving of basins into the bedrock below the fluvial base level; Cook and Swift, 2012; Dürst Stucki and Schlunegger, 2013; Gegg et al., 2021; Gegg and Preusser, 2023; Buechi et al., 2024; Tomonaga et al., 2024). In the study area, these overdeepenings consist of the Birrfeld Basin and its two branch basins, the Hausen Trough and the Gebenstorf-Stilli Trough (GST; Fig. 2; Nitsche et al., 2001; Jordan, 2010; Gegg et al., 2021). These basins were eroded into the bedrock under high subglacial water pressure and became infilled with subglacial diamicts and gravels as well as with (mainly proglacial) lake deposits (Bitterli-Dreher et al., 2007; Graf, 2009a; Gegg et al., 2020, 2021). Forming a connection between the Birrfeld and the HRPC, the Hausen Trough is presumably older than the GST, which lies below the current Reuss/Aare Valley. Erosion of the GST (under strong bedrock control; Gegg et al., 2021) may have enabled abandonment of the HRPC and establishment of the modern drainage configuration (Graf, 2009a; Gegg et al., 2023). The Lower Pleistocene Niederterrasse (Low Terrace) gravel that represents the last glacial cycle, or Birrfeld Glacial (Ivy-Ochs et al., 2008; Graf, 2009a; Preusser et al., 2011; Graf and Burkhalter, 2016), is generally restricted to the present-day river valleys (~310–350 m asl; Graf et al., 2006; Gaar et al., 2019).

Methods

Drilling and field campaign

This project comprises four sites where fully cored scientific drillings were undertaken in 2018 in context of the Quaternary investigation program of the Swiss National Cooperative for the Disposal of Radioactive Waste (Nagra). Three boreholes are located along the axis of the GST: QGBR (47°29′00″N, 8°14′11″E; final depth 123.5 m; Gegg et al., 2019a); QGVO (47°29′43″N, 8°14′18″E; final depth 77.0 m; Gegg et al., 2019b); and QUST (47°30′46″N, 8°14′3″E; final depth 86.4 m; Gegg et al., 2019c). QRIN (47°30′08″N, 8°11′28″E; final depth 52.7 m; Gegg et al., 2018, 2023) was targeted at the HRPC, and is a composite profile of two neighboring boreholes. The 10-cm-diameter drill cores,

~350 m in total, were retrieved by pneumatic hammering and wireline coring using a triple tube core barrel where the core is recovered in a plastic liner, allowing for excellent core quality. All boreholes recovered the entire Quaternary succession and penetrated at least 10 m into the bedrock to guarantee confident bedrock identification. After core recovery, a natural gamma log was acquired. Drilling was further complemented by an extensive field campaign investigating and sampling more than 20 outcrops in the study area (see Fig. 2; Supplementary Table 2), as well as by the integration of lithological logs of previously drilled boreholes collected in Nagra's respective internal database.

Initial core logging and sampling

Bulk density, p-wave velocity, and magnetic susceptibility were measured in 5-mm depth-resolution from the sealed cores prior to opening using a Geotek multi-sensor core logger (MSCL; Schultheiss and Weaver, 1992) at the Institute of Geological Sciences, University of Bern. Afterwards, the cores were split, with one half shielded from light to allow later luminescence sampling, while the other half was further processed. This included photographing with the MSCL-mounted line-scan camera, as well as detailed sedimentological and structural descriptions. Undrained shear strength was determined with a pocket vane tester (max. readout 250 kN/m²) in meter intervals where the sediment was sufficiently cohesive (i.e., rich in fines). Where the sediment was suitably fine grained, we also prepared smear slides and collected bulk sediment samples (~40 g of material) in sub-meter intervals for geochemical analysis. In selected, high-quality core sections at a spacing of ~5 m, we sampled all clasts >15 mm diameter from entire core halves to assess the gravel petrographic composition.

Compositional analysis

Gravel petrography was specifically selected as a tool to distinguish contributions from up to five glacial catchments that are potential sediment sources (Aare, Reuss, and Limmat, potentially also Rhone and Rhine; Figs. 1 and 2). The respective glaciers originated in the High Alps and traversed largely the same major geological units. Consequently, the petrographic spectra of their gravels are generally similar (mostly gray 'Helvetic' limestones; Graf, 2009a). Still, some index lithologies exist (after Hantke, 1978; Graf, 2009a). These include dark porphyritic volcanics and reddish sandstones and conglomerates ('Verrucano') from the area south of Walensee (Den Brok et al., 2021) that are indicators for the Limmat catchment as well as lighter, reddish rhyolitic volcanics ('Windgällenporphyr') indicative of the Reuss catchment (Hantke and Brückner, 2011). Characteristic greenish 'Julier' granites are further indicators of the Rhine catchment (Hantke, 1978; Graf, 2009a).

Greenish volcanogenic 'Taveyannaz' sandstones (Lu et al., 2018) are not index lithologies *sensu stricto* but occur more frequently in gravels from both Reuss and Limmat. Similarly, Graf (2009a) reported notably larger amounts of quartzites in gravels from the Aare (or combined Aare-Rhone) glacier that he attributed to reworking of fan deposits in the Molasse Basin (Schlächter, 1975; Schlunegger et al., 1993; Berger et al., 2005). The Rhone and Rhine systems originate farther into the Alpine interior and thus deliver additionally various ophiolites (Hantke, 1978; Schwenk et al., 2022b). In addition to such rather rare clasts with an index character, non-index lithologies can be very valuable for discrimination of gravel units. This is the case if datasets that comprise a

large number of samples collected arbitrarily and counted by a single operator are evaluated by appropriate statistical means (Graf, 2009a; Gegg et al., 2024).

We identified all clasts >15 mm in diameter from selected core halves, and all clasts >20 mm from volumetric samples collected in the field (including two reference samples each from the tributaries' Niederterrasse gravels for comparison) and attributed them to one of 13 lithology groups (Supplementary Table 1). The minimum clast diameters were chosen so that usually >100 clasts could be obtained per sample (cf., Graf, 2009a; Gegg et al., 2024). We performed endmember analyses on the petrographic data using the R packages EMMAgeo (Dietze and Dietze, 2019; fully unsupervised 'Robust' approach and 'Deterministic' approach where only the number of endmembers is defined by the user) and RECA (Seidel and Hlawitschka, 2015; few input parameters have to be defined by the user). In addition, following log-ratio transformation, the data were evaluated by principal component (PCA, variance-covariance matrix) and cluster analysis (Ward's method, Euclidean distance matrix) in Past 3 (Hammer et al., 2001). In sand- or fine-grain-dominated sections, the water content (WC) of bulk sediment samples was measured by weighing and freeze-drying. Geochemical composition (i.e., total inorganic carbon [TIC], total organic carbon [TOC], total sulfur [TS], and total nitrogen [TN]) was determined by combustion of small sample amounts (few mg) and combustion gas analysis in a thermal conductivity detector (Boyle, 2001; Meyers and Teranes, 2001). This was done using a Thermo Scientific Flash 2000 Smart elemental analyzer (details on the procedure in Krotz and Giazzi, 2018). TIC was converted to CaCO_3 content by multiplication with a stoichiometric factor of 8.33 ($= M_{\text{CaCO}_3}/M_C$).

2D seismic acquisition

Three high-resolution 2D reflection seismic lines were acquired on the Ruckfeld gravel plain by Nagra in 2016: 16-QAU_23, 16-QAU_24 (both oriented SW–NE), and 16-QAU_25 (oriented SE–NW; Fig. 2). The seismic lines are 1.5–2.2 km long, and were recorded using a combination of Inova Univib vibrators and explosives excited every 5 m as sources, and a geophone spacing of 2.5 m. The Mesozoic bedrock and the overlying Quaternary strata were imaged in time domain. The migrated data were visualized in IHS KingdomSuite and DMNG SeiSee and interpreted with respect to available drilling and surrounding regional-scale reflection seismic data (Madritsch et al., 2013).

Results

Lithostratigraphy

Base of Quaternary

All drillings into the GST reached the pre-Quaternary bedrock (QGBR: 111.5 m depth at 225.8 m asl; QGVO: 64.9 m depth at 266.1 m asl; QUST: 76.0 m depth at 255.2 m asl; Figs. 3–5; Gegg et al., 2019a–c, 2021). In the overlying Quaternary strata (Fig. 6), and in a variety of outcrops in the study area, we distinguish four lithofacies associations (LFA 1–4), which are characterized in the following. A detailed description of the succession recovered at QRIN is provided in Gegg et al. (2018, 2023).

LFA 1: basal diamicts

At the base of the GST infill, we encountered diamicts overlying the bedrock (LFA 1). These are soft to stiff, massive, and 2.7 m thick

in QGBR, 0.7 m thick in QGVO, and 1.3 m thick in QUST. The diamicts consist of mostly angular gravel clasts and cobbles embedded in a yellowish gray to olive (partly blueish in QGBR, as a result of reworking of an underlying paleokarst infill; Gegg et al., 2020) and clayey to sandy matrix. The diamicts are generally relatively poor in matrix and partly clast-supported (Fig. 6A). In QGBR and QGVO, LFA 1 contains occasional striated clasts, which were not encountered in QUST, where instead soft clumps occur that might be reworked marl bedrock. Basal diamicts are characterized by low water content (< 15%), intermediate to high bulk density (2.0–2.5 g/cm³), and intermediate gamma signals (30–50 API, 50–70 API in QGBR). Magnetic susceptibility shows distinct peaks, with the exception of QUST, where the signal within the basal diamict is generally low. These peaks may relate to individual clasts, but we also occasionally observe fragments of the drill bit or core catcher, which create strong artificial peaks.

LFA 2: sandy gravels

Different units of sandy gravels occur in all studied cores (LFA 2) and generally consist of dm- to m-scale beds that are frequently graded and of yellowish to brownish gray color. Gravels overlying the basal diamicts in QGVO (64.2–55.8 m depth) and QUST (especially the bottom ~20 m) are mostly poorly sorted with a significant silt and sand component (LFA 2a, Fig. 6B), and contain massive or crudely bedded sand intercalations up to ~1 m thick. In QGVO, these basal gravels also contain a few striated clasts, as does an interbed of poorly sorted gravel with cobbles at 28.3–26.5 m depth (Fig. 6I). The shallower gravels in QGBR (23.6–8.0 m depth), QGVO (17.4–0.0 m), and QUST (top ~20 m) consist of both poorly sorted intervals and well-sorted open-framework gravels as well as pure dm-scale sand layers, sometimes as fining-upward sections (LFA 2b, Fig. 6C, G). Individual clasts are predominantly rounded. LFA 2 deposits generally have a high density (~2.5 g/cm³), low gamma signals (frequently < 25 API), and distinct, natural or artificial (see above) peaks in magnetic susceptibility. Water contents range from ~15% to 30%.

Our study includes a variety of outcrops in active and abandoned gravel pits and artificial or natural cuts (see Fig. 2). The respective deposits have been attributed to the Tiefere Deckenschotter, Hochterrasse, and Niederterrasse (Matousek et al., 2000; Graf et al., 2006). Coordinates and brief descriptions of the studied outcrops are given in Supplementary Table 2, together with a list of samples collected in the field. At all sites, sandy gravels occur at a variety of exposure extents and conditions. In some larger outcrops, a complex sedimentary architecture can be observed, including distinct bedding planes, cross-bedded gravel and sand lenses, and graded sections. The gravels in several exposures are overlain by glaciogenic diamicts.

LFA 3: massive and bedded sands and silts

The successions of QGBR (108.8–23.6 m depth) and QGVO (55.8–17.4 m depth) largely consist of soft, yellowish to olive gray silty sands (LFA 3) that occur in three different subunits (LFA 3a–c). Whereas the sands of LFA 3a are massive (Fig. 6D), those of LFA 3b exhibit a well-developed and sometimes rhythmic bedding (Fig. 6E). LFA 3b is characterized by 1–5 cm thick, olive-gray, coarse layers alternating with up to 2-cm-thick, lighter yellowish gray, silt-dominated layers. These bedded deposits are frequently deformed, including drilling-related drawdowns at the core edges, but also convolution of the layering that may be unrelated to

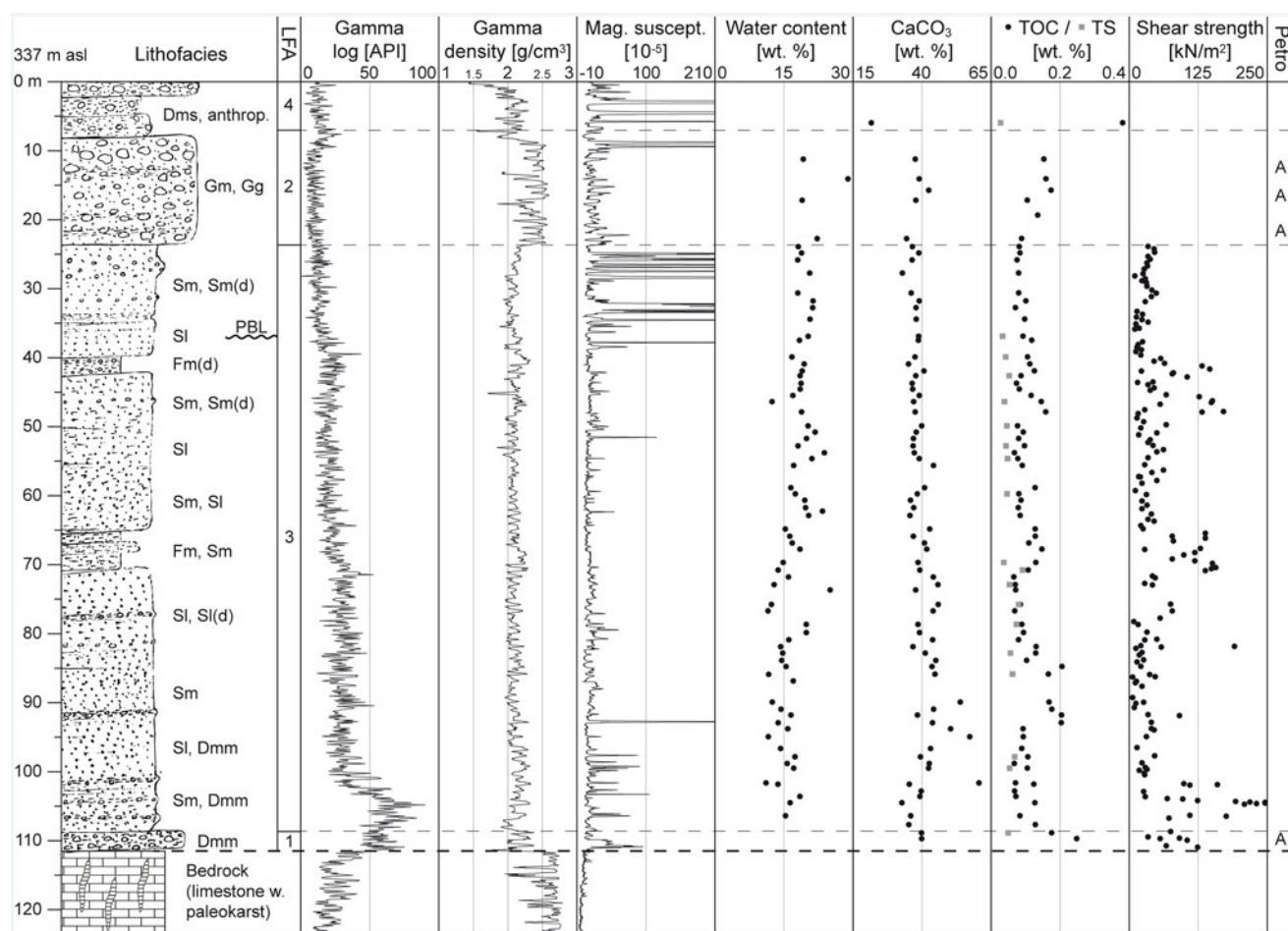


Figure 3. Composite plot of borehole QGBR. Lithofacies codes are based on Miall (1977) and Eyles et al. (1983): D = diamict, S = sand, F = fines, G = gravel, -m = massive, -mm = matrix-supported and massive; -ms = matrix-supported and stratified; -l = laminated, -g = graded, (d) = with dropstones. LFA = lithofacies association; PBL = lowest local Pleistocene base level (300 m asl; Graf, 2009a); anthrop. = anthropogenic; Petro = dominant gravel petrographic signal (A = Aare, see Figures 7 and 8).

drilling deformation but caused, for example, by slumping. Layers with infrequent dispersed gravel clasts occur throughout QGBR, and in the top half of QGVO (above 35 m depth). QGBR further recovered occasional dm- to m-scale interbeds that are silt dominated and, both below 80 m and above 45 m depth, frequently contain outsized clasts (LFA 3c, Fig. 6F). Such a diamictic section also occurs at the top of LFA 3 in QGVO (22.3–17.4 m depth, Fig. 6H).

Densities of LFA 3 sediments are generally intermediate ($2.0\text{--}2.2\text{ g/cm}^3$), and magnetic susceptibility is low, with the exception of individual peaks especially in the top ~15 m of QGBR, which likely relate to outsized clasts. In QGBR, pocket vane testing revealed three distinct intervals (~40–50 m, ~65–70 m, and ~100–110 m) where shear strength is elevated from background values below 100 kN/m^2 up to 170 kN/m^2 , and in the deepest interval to $>250\text{ kN/m}^2$ (Fig. 3). These correspond to occurrences of LFA 3c. The upper LFA 3 section of QGVO (26.4–17.4 m) shows upwards-increasing shear strength from ~20 to ~140 kN/m^2 (Fig. 4). Gamma signals are low ($< 25\text{ API}$) throughout QGVO and in the upper part of QGBR, where they increase downward to $> 50\text{ API}$. Water contents scatter between 15% and 30% in QGVO and show an upward-increasing trend from 10–15% to 15–20% in QGBR.

LFA 4: waste deposit

At the top of the succession, QGBR recovered 8.0 m of olive gray to black silty diamicts (LFA 4). Brick and metal fragments identify these as anthropogenic waste deposits, which are not of further relevance to this study (cf., Graf et al., 2006).

Sediment composition

Geochemistry

Geochemical data are shown on Figures 3 and 4. LFA 3 sediments of QGBR and QGVO are characterized by TOC and TS values generally below 0.2% and 0.1%, respectively, while nitrogen was not detectable. CaCO_3 content is typically ~40% but drops abruptly to ~30% above the LFA 2 interbed of QGVO at 26.5 m depth.

Gravel petrography

Gravel petrographic data are provided in Supplementary Tables 3 and 4 (drill cores, including QRIN, and outcrops, respectively). Gray limestone clasts are generally most abundant, representing one-half to two-thirds of most samples, followed by clastic sedimentary rocks (sandstones and conglomerates; less than one-third), quartzites *sensu lato* (including vein quartz, cherts, and radiolarites; less than one-third), and crystalline clasts ($< 10\%$). An

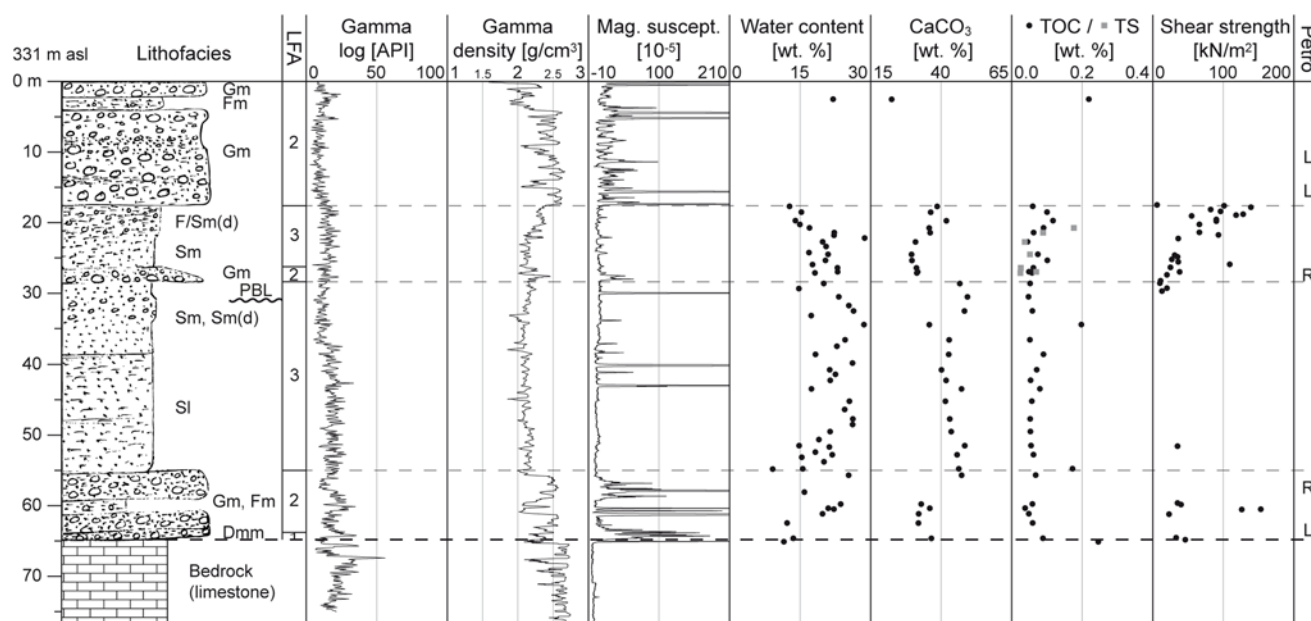


Figure 4. Composite plot of borehole QGVO. Lithofacies codes are based on Miall (1977) and Eyles et al. (1983): D = diamict, S = sand, F = fines, G = gravel, -m = massive, -mm = matrix-supported and massive, -l = laminated, (d) = with dropstones. LFA = lithofacies association; PBL = lowest local Pleistocene base level (300 m asl; Graf, 2009a); Petro = dominant gravel petrographic signal (L = Limmat, R = Reuss, see Figures 7 and 8).

exception is one sample from the cover diamicts of QRIN (6.5–7.5 m depth), which differs from all other samples as it contains > 50% (as opposed to < 20%, and often < 5%) of light beige limestones of the JFTB (Gegg et al., 2023). These limestones represent local erosion and reworking instead of indicating the glacier source area and were thus omitted from the following analyses.

The results of the automatic endmember (EM) analyses using the EMMAgeo ('Robust' and 'Deterministic' approaches; Dietze and Dietze, 2019) and RECA (Seidel and Hlawitschka, 2015) R packages are shown on Supplementary Figure 1. The automatic, 'Robust' EMMAgeo-approach modeled three EMs, corresponding to the threefold confluence situation of Aare, Reuss, and Limmat (Fig. 2), consequently three EMs were also used for all analyses where their number has to be specified by the user. For RECA, we used a convexity threshold of -6, and weighing exponent of 1, as recommended by Seidel and Hlawitschka (2015). The model performance was tested with assumed true EM taken from the Niederterrasse of the respective river valleys. The contributions of these reference samples were best reproduced by the Robust EMMAgeo model; therefore, we use the results of this approach for further interpretation (Fig. 7).

An Aare-dominated petrography, characterized mainly by high quartzite contents (EM1), is thus inferred for all samples of QGBR and QRIN, while the samples of QGVO and QUST contain more prominent Reuss/Limmat components (higher limestone contents, EM2 and EM3, respectively; Fig. 7). Specifically, most samples of QGVO and QUST are dominated by a Limmat signal (especially rich in non-siliceous limestones), except mainly for the gravel interbed of QGVO at ~28 m depth and the interval at ~40–25 m depth of QUST, which show a Reuss-dominated petrography. In accordance with Graf (2009a), our data further indicate a rather variable-mixed Aare/Reuss provenance for the Habsburg Gravel, and a well-distinguishable Reuss/Limmat provenance for the Remigen Gravel in the HRPC. The composition of the Hochterrasse farther downstream the Aare Valley indicates mixed

provenances. A Reuss/Limmat-dominated petrography is inferred for two samples of the Tiefer Deckenschotter of Bruggerberg, in agreement with the findings of Graf (1993). These results are in good agreement with principal component (PCA, Fig. 8) and cluster analyses (Supplementary Fig. 2). In the PCA, inferred Aare provenance corresponds mainly to a high PC1 score (i.e., frequent quartzites), Limmat provenance to a high PC2 score (i.e., frequent limestones), and Reuss provenance to a low score of both components (i.e., frequent sandy and siliceous limestones; Fig. 8). Interestingly, the Niederterrasse samples, assumed to represent true EM, do not lie at the most extreme positions in the PCA plot.

The Limmat provenance is especially well supported by index lithologies (> 1% red sandstones, presence of non-rhyolitic volcanics; Supplementary Tables 3, 4). Noteworthy evidence for contributions from the Rhine and Rhone catchments in the shape of the according index lithologies was not identified.

Seismic data

The subsurface of the Ruckfeld comprises two main seismic facies (SF A and SF B; Fig. 9). The lower SF A consists of horizontal to slightly southward-dipping continuous reflections with moderate to high amplitudes that are in several places affected by smaller (i.e., kinks) and larger dislocations (i.e., visible offsets). At ca. 0.2 s two-way travel time (TWT), a sharp horizontal boundary forms an angular unconformity. The strata above, SF B, are characterized by mostly lower-amplitude, frequently discontinuous and hummocky reflections. On lines 16-QAU_23 and 16-QAU_24, a relatively continuous and distinct internal horizontal reflection that subdivides SF B can be observed. While the upper part of SF B is largely seismically transparent, several discontinuous units of high-amplitude reflections as well as smaller-scale discontinuities and dislocations occur in the lower part.

Discussion

Evolution of the overdeepened Gebenstorf-Stilli Trough (GST)

Subglacial erosion and onset of sedimentation

The GST is one of two northward extensions of the Birrfeld Basin and has been excavated over the course of an ice advance over the Birrfeld and the JFTB along the present-day lower Reuss Valley (Fig. 2; Graf, 2009a; Gegg et al., 2021). Gegg et al. (2021) showed that trough formation was strongly controlled by the specific local bedrock lithology (incision efficiency and depth), and potentially structure (localization). After its incision, the GST was filled with diverse deposits reflecting its development after incision (Fig. 10).

Overlying the basal bedrock unconformity, the Gebenstorf Trough diamict comprises a few meters of massive diamict and/or gravel (LFA 1, 2). Such deposits occur commonly at the base of overdeepening-fill successions, but their nature and formative process have been disputed (e.g., Gegg and Preusser, 2023). Striated clasts in QGBR and QGVO identify the diamict as an ice-derived deposit. In QGBR, the lowermost 0.5 m are stiff and compact, which indicates direct loading by glacier ice. In contrast, the other basal diamicts are looser and softer. This is characteristic rather of water-lain glaciogenic diamicts (i.e., deposits originating mainly from melt-out and reworking by subglacial mass movements and/or subglacial water flow) than of overconsolidated subglacial tills dominated by processes such as lodgment (Schluchter, 1997; Evans et al., 2006). The relatively matrix-poor, sometimes clast-supported character of the Gebenstorf Trough diamict is a further indicator of modification by flowing water through winnowing of fines (e.g., Boulton and Paul, 1976). We therefore refrain from the term 'till' and use the purely descriptive term 'diamict' (although the diamict probably contains some isolated occurrences of actual till sensu Eyles et al., 1983, like at the very base of the QGBR infill). We explain the properties of this diamict, as well as its comparably small thickness (cf., Wyssling and Wyssling, 1978; Pomper et al., 2017; Buechi et al., 2018, 2024; Schwenk et al., 2022a) by efficient flushing of debris from the glacier base during erosion and ice occupation of the GST. Although only a little material was available, contributions from the catchments of Aare, Reuss and Limmat could be identified in petrography samples of the Gebenstorf Trough diamict (Figs. 3–5, 7, 8). The combined drainage area of these three catchments delivered large amounts of melt water that passed through the narrow cross-section of the GST, while its sediment load may have been retained to a large degree by the Birrfeld Basin and overdeepened areas farther up in the tributary catchments, especially that of the Reuss River (Alley et al., 1997, 2019; Pietsch and Jordan, 2014; Gegg et al., 2021). Deposition of the Gebenstorf Trough diamict reflects the cessation of this efficient flushing and thus the transition to (sub-)glaciolacustrine conditions of the ice-decay phase rather than the pleniglacial phase.

Lacustrine phase

Above the basal diamicts, the several-decameter-thick massive to bedded Gebenstorf Sand (LFA 3) represents the majority of the overdeepening infill (Fig. 10; to the north it interfingers with coarser delta deposits, see below). This sand is interpreted as a glaciolacustrine deposit based on its uniform, entirely detrital sedimentology, very low content of organic material with TOC generally less than 0.2%, and no macro- or microfossils encountered (cf., Graf, 2009a; Anselmetti et al., 2010; Dehnert et al., 2012). The dominant preservation of sedimentary bedding further indicates a cold, inorganic environment without burrowing organisms

throughout its deposition (Zolitschka et al., 2015). Dispersed out-sized fragments are interpreted as melt-out debris from icebergs or from a floating, decaying glacier tongue. A distinct glacially derived component, especially in the basal Gebenstorf Sand, is further suggested by elevated gamma signals (> 50 API), which indicate increased, reworked clay mineral content (Serra and Sulpice, 1975).

In contrast to the majority of other records of overdeepened basin fills that also comprise thick units of basinal fines (e.g., Schluchter, 1989; Dehnert et al., 2012; Buechi et al., 2018, 2024), that of the GST is entirely sand-dominated. A finer-grained Reusstal Clay occurs only south of the studied section, and stratigraphically higher up (Fig. 10; Graf et al., 2006; Graf and Burkhalter, 2016). This clay represents the continuation of the fining-upward succession in the Gebenstorf-Stilli Trough (Buechi et al., 2024) that was originally probably also present, but later eroded, in the GST, which would correspond to an ancient lake level of at least ~ 330 m asl. The preserved sandy infill of the trough indicates a comparatively glacier-proximal setting with high sediment input from three Alpine catchments. Deformed and/or massive LFA 3 sections point towards instability due to rapid deposition and consequent soft-sediment deformation but could also be related to drilling (Mills, 1983; Pisarska-Jamroz and Weckwerth, 2013). However, especially in QGBR, the majority of the basin infill is well bedded, with darker, sand-dominated layers alternating with lighter and thinner, silt-dominated layers (Fig. 6E). Such rhythmic alternations are encountered throughout the entire succession in relatively constant thickness of a few cm. They are tentatively interpreted as clastic varves (Peach and Perrie, 1975; Leonard, 1986; Zolitschka et al., 2015), and suggest an emplacement of the lacustrine sequence during a single, continuous phase over few thousand years at most. This interpretation is supported by the generally uniform sedimentology as well as the only slightly and gradually changing geochemistry, as reflected by the CaCO_3 and TOC content (Fig. 3). However, repeatedly occurring intervals that are distinctly enriched in fines (and consequently of higher shear strength; Fig. 3) and/or contain dropstones may indicate decadal- to centennial-scale oscillations of a glacier front farther south that influenced sediment input into the basin (as observed elsewhere, e.g., Smedley et al., 2017; Chiverrell et al., 2018).

Origin of gravels at the distal trough end

Overlying the Gebenstorf Trough diamict, QUST recovered exclusively sandy gravel with occasional sand interbeds. Logs of several dozen previous boreholes in the study area confirm that the distal GST infill is generally gravelly (Stilli Delta Gravel; Fig. 10). Based on seismic and drilling data, we assume a total volume of these coarse-grained sediments of $\sim 5 \times 10^7 \text{ m}^3$ (Gegg et al., 2021). Two groundwater exploration boreholes ($47^\circ 30' 20'' \text{N}$, $8^\circ 14' 11'' \text{E}$ and $47^\circ 30' 39'' \text{N}$, $8^\circ 14' 04'' \text{E}$) further reveal an interdigitation of the Stilli Delta Gravel with the Gebenstorf Sand, and thus a simultaneous deposition of both facies (Fig. 10). The distal gravels of the GST must have been emplaced in a (glacio-)deltaic setting, which agrees well with the thick-bedded and frequently graded architecture (e.g., Gilbert et al., 2017).

The petrographic composition of the gravels throughout QUST is dominated by far-travelled, Alpine lithologies ($\geq 90\%$; see Supplementary Table 3, Gegg et al., 2021), precluding an origin from local erosion in the Mesozoic rocks cropping out in the vicinity. Counterintuitively, the Stilli Delta Gravel must have been deposited from upstream by glacial and/or glaciofluvial transport toward the distal trough end. Near the trough base, a (sub)glacial origin of the coarse-grained material, being transported towards

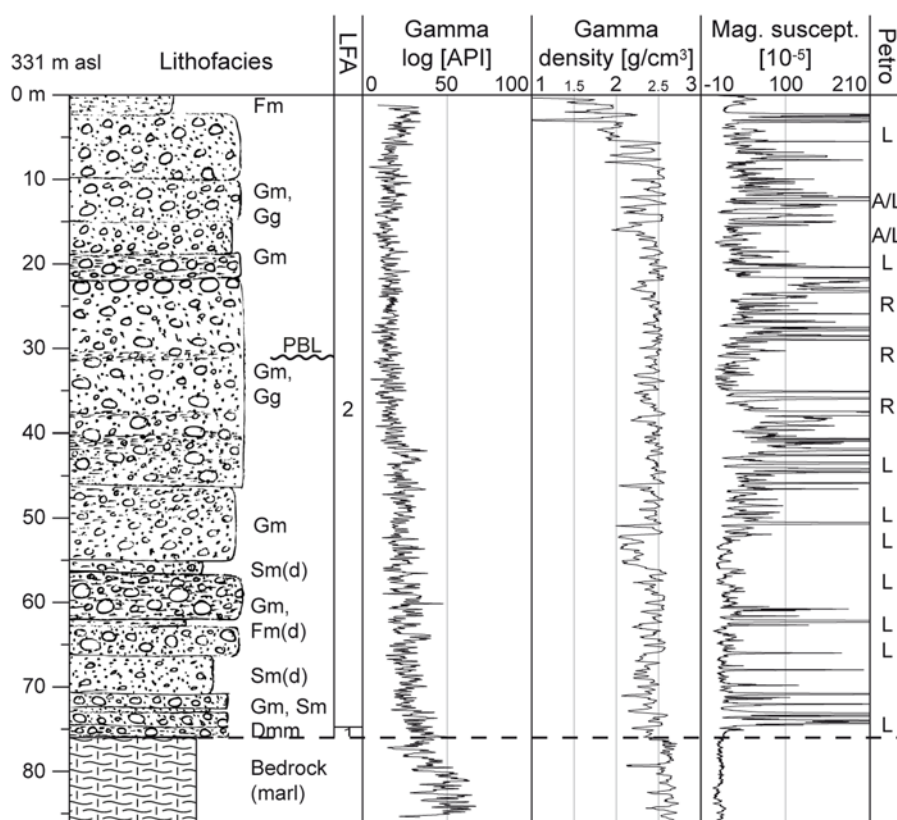


Figure 5. Composite plot of borehole QUST. Lithofacies codes are based on Miall (1977) and Eyles et al. (1983): D = diamict, S = sand, F = fines, G = gravel, -m = massive, -mm = matrix-supported and massive; -g = graded, (d) = with dropstones. LFA = lithofacies association; PBL = lowest local Pleistocene base level (300 m asl; Graf, 2009a); Petro = dominant gravel petrographic signal (A = Aare, L = Limmat, R = Reuss, see Figures 7 and 8).

the terminal slope of the overdeepening by water flow along the glacier base, cannot be excluded (Mullins and Hinchey, 1989). However, farther up the sequence, the gravels interfinger with well-sorted and well-bedded lacustrine sands that are not compatible with an overlying glacier. The petrography of the Stilli Delta Gravel in QUST shows a strong Limmat signal (Figs. 7 and 8), indicating that it was delivered from the Limmat catchment laterally into the overdeepening, forming a gravel delta at the distal trough end, in front of the lacustrine sands.

This hypothesis is plausible considering the bedrock morphology: large parts of the Aare and Reuss valleys farther south, for example the Birrfeld Basin (Fig. 2), are overdeepened and therefore prone to retain coarse-grained sediment. In contrast, overdeepened sections in the Limmat Valley occur only ~20 km upstream of the study area (Jordan, 2010; Pietsch and Jordan, 2014), and any coarse-grained material delivered into the valley in between, for example as melt-out during ice retreat, likely would have been transported into the GST. This input of Limmat-derived material, however, probably did not occur at its present-day confluence point with the Aare but farther north, at the exit of the Surb Valley (Fig. 2), as demonstrated by Graf (2009a) based on gravel petrographic analyses.

Glacial re-advance

In contrast to the seemingly continuous sedimentology in QGBR and QUST, the Gebenstorf Sand is sharply overlain by a ~2-m-thick gravely intercalation (Vogelsang Gravel) in QGVO at ~28 m depth (Figs. 6I and 9). This interbed coincides with an abrupt up-section decrease in CaCO_3 and a significant increase in fines as well as outsized gravel clasts (Fig. 4) that signal a drastic change in the basin sedimentation. A striated dark limestone clast at the top

of the gravel bed together with the diamictic character of the overlying LFA 3 deposits (Vogelsang Sand; Fig. 10) indicates renewed glacier proximity. This points towards a re-advance very close to, and possibly over, the site of QGVO (although a reworking of older deposits in the vicinity, for example by a mass movement affecting the Tiefere Deckenschotter at Bruggerberg, cannot entirely be excluded, cf. Fig. 11). Although this facies change also is observed in several previous boreholes near QGVO, it is missing in the record of QGBR, which is located few km farther upstream, where no clear indication for a renewed ice contact is found. Therefore, it would seem plausible that the sedimentological break in QGVO is the result of a lateral advance into the GST that did not reach the site of QGBR. However, its petrographic composition (Figs. 7 and 8) indicates that the Vogelsang Gravel has a rather Reuss-dominated petrography, indicating an axial advance along the Reuss Valley and over the GST, thus affecting also QGBR. Its petrographic composition further allows identification of the Vogelsang Gravel in the record of QUST: between ~25 and ~40 m depth, the strong Limmat signal that is otherwise characteristic for the gravels in this borehole is interrupted by a phase of deposition of Reuss-facies gravels (Figs. 5, 7, 8). This strongly suggests a later advance of the Reuss glacier into the GST that carved out a second inlaid basin that was quickly filled during its retreat (Fig. 10). Whether this re-advance occurred during the same glacial cycle and only briefly after deposition of the underlying Gebenstorf Sand, or after a considerable hiatus, cannot be determined from the sedimentary facies.

Post-lacustrine phase

The (glacio-)lacustrine infill of the GST is sharply truncated and overlain by ~15 m of Late Pleistocene Niederterrasse gravel (Fig. 10; Graf et al., 2006). Interglacial deposits and/or soil have

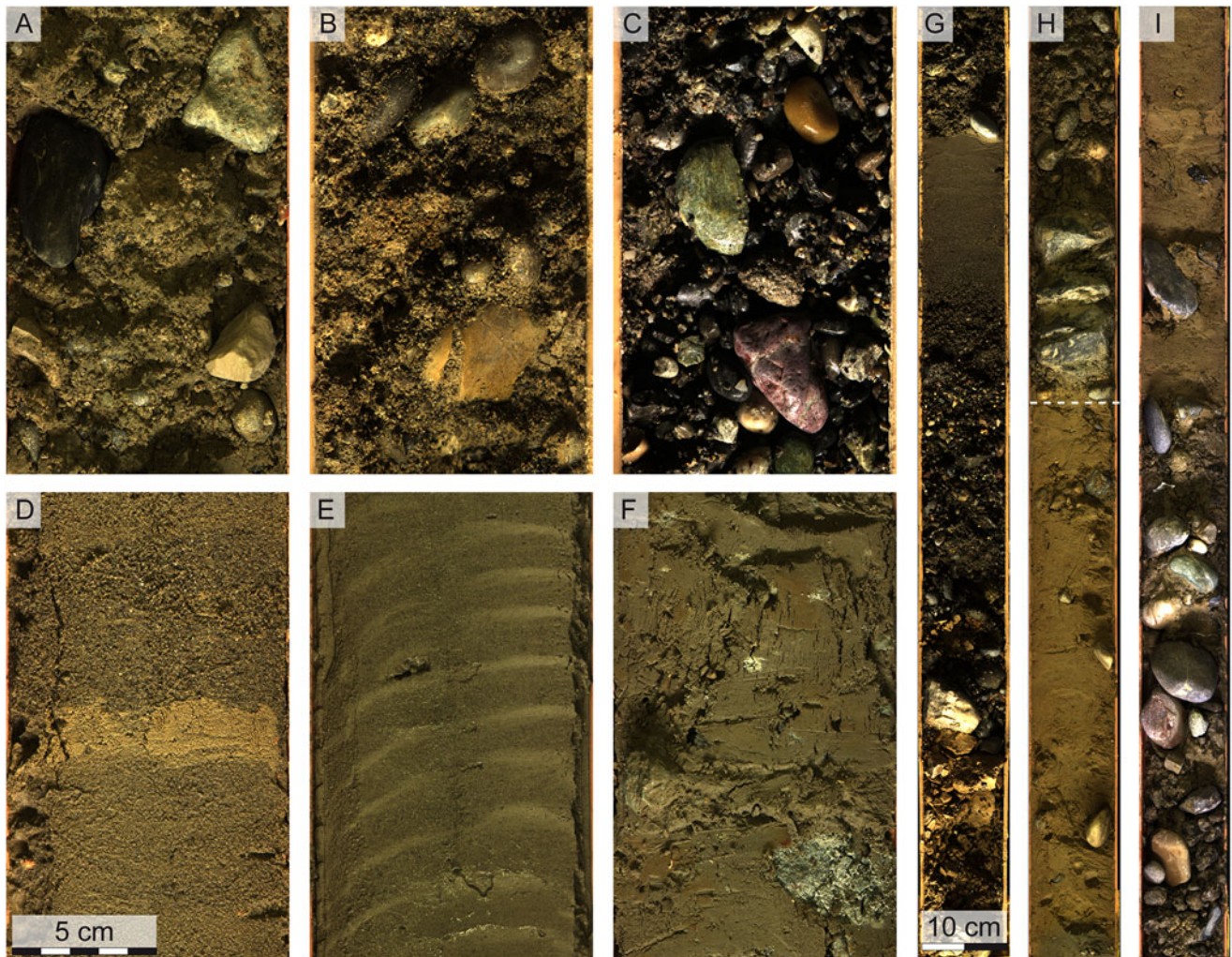


Figure 6. Core photos representing lithofacies associations 1–3 (LFA 1–3); waste deposit LFA 4 not displayed; width of all images is 10 cm. (A) LFA 1, massive sandy diamict with (sub-)angular clasts at the base of QGVO (~64.4 m depth). (B) LFA 2a, poorly sorted, sand-rich gravel with (sub-)rounded clasts (QUST, 65.6 m). (C) LFA 2b, moderately sorted, fine to medium gravel (QUST, 16.5 m). (D) LFA 3a, massive sand with fine-grained interbed (QGVO, 34.4 m). (E) LFA 3b, silty sand with rhythmic bedding (QGBR, 55.6 m). (F) LFA 3c, clayey sand with dispersed clasts, diamictic (QGBR, 101.9 m). (G) Fining-upward cycle within LFA 2, from cobble to sand size (QUST, 13–14 m). (H) Boundary between LFA 2 (top) and 3 (bottom; QGVO, 17–18 m). (I) Coarse LFA 2 interbed within LFA 3 (QGVO, 27–28 m). Photos of all core sections are provided in Gegg et al. (2019a–c).

not been recovered in between, although the top of the underlying LFA 3 in QGVO shows a slightly more brownish color that may be due to temperate weathering (Fig. 6H). The Niederterrasse has a prevailing Aare signature at QGBR, a Limmat signature at QGVO, and a mixed Aare-Limmat signature at QUST (Figs. 7 and 8). Borehole data indicate that the Niederterrasse fills distinct channels incised into the glaciolacustrine deposits (Fig. 10; Gegg et al., 2021). Several previous boreholes at the northern end of the GST recovered limestone blocks at ~320 m asl (317.2 m asl or 13.9 m depth in QUST), which indicates an important event horizon within the lower part of the Niederterrasse. Finally, anthropogenic waste in the cover diamicts of QGBR identifies this material as a recent waste deposit (Graf et al., 2006).

Evolution of the Habsburg-Rinikerfeld Palaeochannel

At the base of the HRPC, borehole QRIN recovered ~3.5 m of an overconsolidated subglacial till that is matrix-rich but also contains frequent striated clasts (Rinikerfeld Basal Till; Gegg et al., 2023). It

is overlain by ~2 m of poorly sorted gravels, and both have the same Aare-dominated petrographic composition (Figs. 7, 8, 11). They are in turn overlain by a lacustrine sequence (Rinikerfeld Paleolake) that develops from an ice-contact toward a periglacial and lastly a cold-temperate setting. Geotechnical evidence suggests that this sequence, which is capped by colluvial deposits, was overridden by a later ice advance (Mueller et al., 2020; Gegg et al., 2023).

The main depositional units encountered in the HRPC however are the Habsburg Gravel and Remigen Gravel, two units attributed to two separate Middle Pleistocene glaciations (Fig. 11). These glaciofluvial units can be distinguished based on their petrographic compositions. The older Habsburg Gravel has a clear Aare (/Reuss) provenance (Figs. 7 and 8; Bitterli-Dreher et al., 2007; Graf, 2009a). Based on petrographic data, we thus identify the gravel underlying the paleolake in QRIN as Habsburg Gravel, and we further show that the Rinikerfeld Basal Till has the same Aare-dominated composition (Fig. 7). The two depositional facies, till and gravel, could represent two different glacial

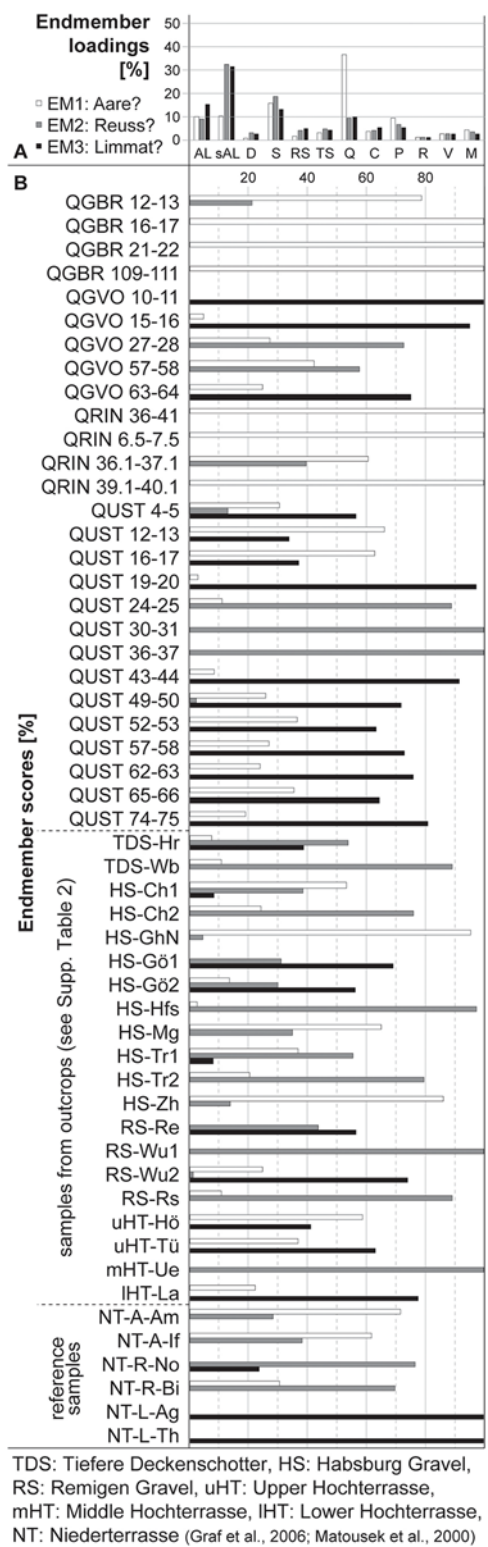


Figure 7. Results of endmember (EM) modeling using the Robust EMMA approach of Dietze and Dietze (2019). (A) The model produces a quartz-rich EM (EM1, white) that is tentatively correlated with an Aare input (as suggested by Graf, 2009a), a siliceous Alpine limestone-rich EM (EM2, gray) tentatively correlated with a Reuss input, and a third EM rich in non-siliceous Alpine limestone (EM3, black) that is tentatively correlated with a Limmat input. For lithology group abbreviations, see Figure 8 or Supplementary Table 2. (B) EM scores of individual samples indicate contributions from the respective catchments. The correlations are supported by the EM scores of reference samples from the Late Pleistocene Niederterrasse (bottom; NT-A-x from the Aare, NT-R-x from the Reuss, and NT-L-x from the Limmat Valley). The calculated EM scores generally agree well with principal component analysis (PCA; Figure 8) and clustering results (Supplementary Figure 2), as well as previous studies.

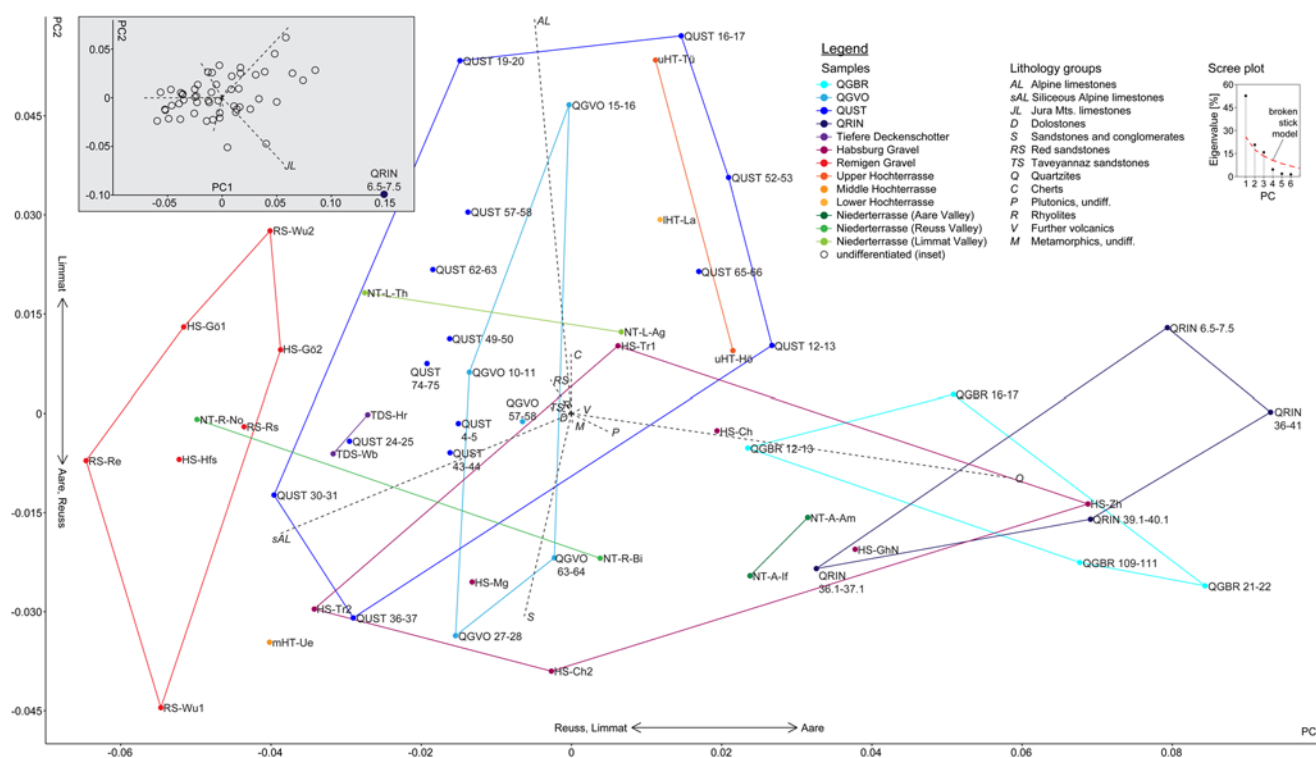


Figure 8. Results of principal component analysis (PCA) excluding locally derived limestones from the Jura Mountains. Component 1 (PC1) distinguishes samples with high quartzite content (high PC1) from samples with a high content of siliceous Alpine limestones (low PC1); both lithology groups have a correlation coefficient of -0.64 . High PC1 scores indicate a relatively increased Aare contribution, while lower PC1 scores indicate a relatively increased Reuss/Limmat contribution, as suggested by reference samples (green) from the Niederterrasse of the respective river valleys (Graf, 2009a). PC2 separates samples predominantly rich in Alpine limestones from samples rich in sandstones (correlation coefficient -0.29), indicative of increased Limmat and Aare/Reuss contributions, respectively. Inset: PCA of the full petrographic dataset including Jura Mountains limestones clearly separates one sample from the cover diamicts of QRIN (QRIN 6.5–7.5) from all other samples based on its high content of these rocks ($> 50\%$ as opposed to $< 20\%$; see also Gegg et al., 2023).

cycles, as has previously been assumed, whose ice advances shared the same provenance. However, it appears more likely that both were deposited by the same glacier and during the same glaciation, and that this glaciation advanced into and possibly well beyond the Rinikerfeld.

The Remigen Gravel occurs locally on top of the Habsburg Gravel, sometimes in the shape of an incised channel fill (Figs. 11 and 12; Graf, 2009a, Preusser et al., 2011) and has a Reuss-/Limmat-dominated petrography. We thus identify deposits north of Brugg (Hansfluhsteig, HS-Hfs; Fig. 2) that were previously attributed to the Habsburg Gravel (Graf et al., 2006) as Remigen Gravel based on their composition (Figs. 6 and 7). The same applies to gravels cropping out in the Götschel pit farther south (HS-Gö1/-2; Habsburg Gravel in Graf et al., 2006, but already attributed to the Remigen Gravel in Graf, 2009a). Previous boreholes recorded intercalated diamictic deposits within the Remigen Gravel east of the former gravel pit at Alpbeg (RS-Re). These were identified as tills (Remigen Till 1) by the site geologist and thus indicate an intermittent ice advance at least to the northern margin of the Rinikerfeld during deposition of the Remigen Gravel (Fig. 11).

The Remigen Gravel also was overridden by a later ice advance, as indicated by a till cap exposed in the Alpbeg pit (Remigen Till 2) as well as by glaciotectionic deformations and crushed clasts in the Götschel pit. Evidence of ice contact in the form of striated clasts and entire polished conglomerate blocks is also encountered at the top of the Upper Hochterrasse in the Hönger gravel pit farther

north (uHT-Hö, Fig. 2; see also Bugmann, 1961; Graf, 2009a). This unit was interpreted as a correlative of the Habsburg Gravel by Graf (2009a), but with a different, mixed Aare/Reuss/Limmat/Rhine petrography, the latter being supported by our compositional data (Figs. 7 and 8). Based on the outcrop elevations and the ice contact at the top of both units, we suggest that the Upper Hochterrasse might correlate rather to the Remigen Gravel, while the elevation of the Habsburg Gravel corresponds better to the Middle and Lower Hochterrasse (Fig. 12). A paleosol between gravel and till remnants at the Hönger outcrop that was suggested by Bugmann (1961) could not be confirmed.

Concerning petrographic compositions, it is noteworthy that a considerable number of samples from both HRC and GST have more 'extreme' gravel spectra (i.e., higher PC scores) than the assumed true EMs from the Niederterrasse of Aare, Reuss, and Limmat (Fig. 8). This may in part be due to the small number of reference samples that do not represent the variability of the true EMs well. Higher amounts of quartzites compared to the Aare reference samples could further be explained by post-depositional weathering of less-resistant clasts, which likely applies to the sample from Haselloch (HS-Zh, Supplementary Table 4). For the fresher-looking samples from QGBR and QRIN, this is probably not the case. Following Graf (2009a), their enrichment of quartzites might indicate a relatively higher rate of reworking of material from molasse-fan deposits in the proximal foreland (Schlunegger et al., 1993; Berger et al., 2005) compared to the supply rate of new debris from the Alps (see also Schlüchter, 1975). However, the opposite

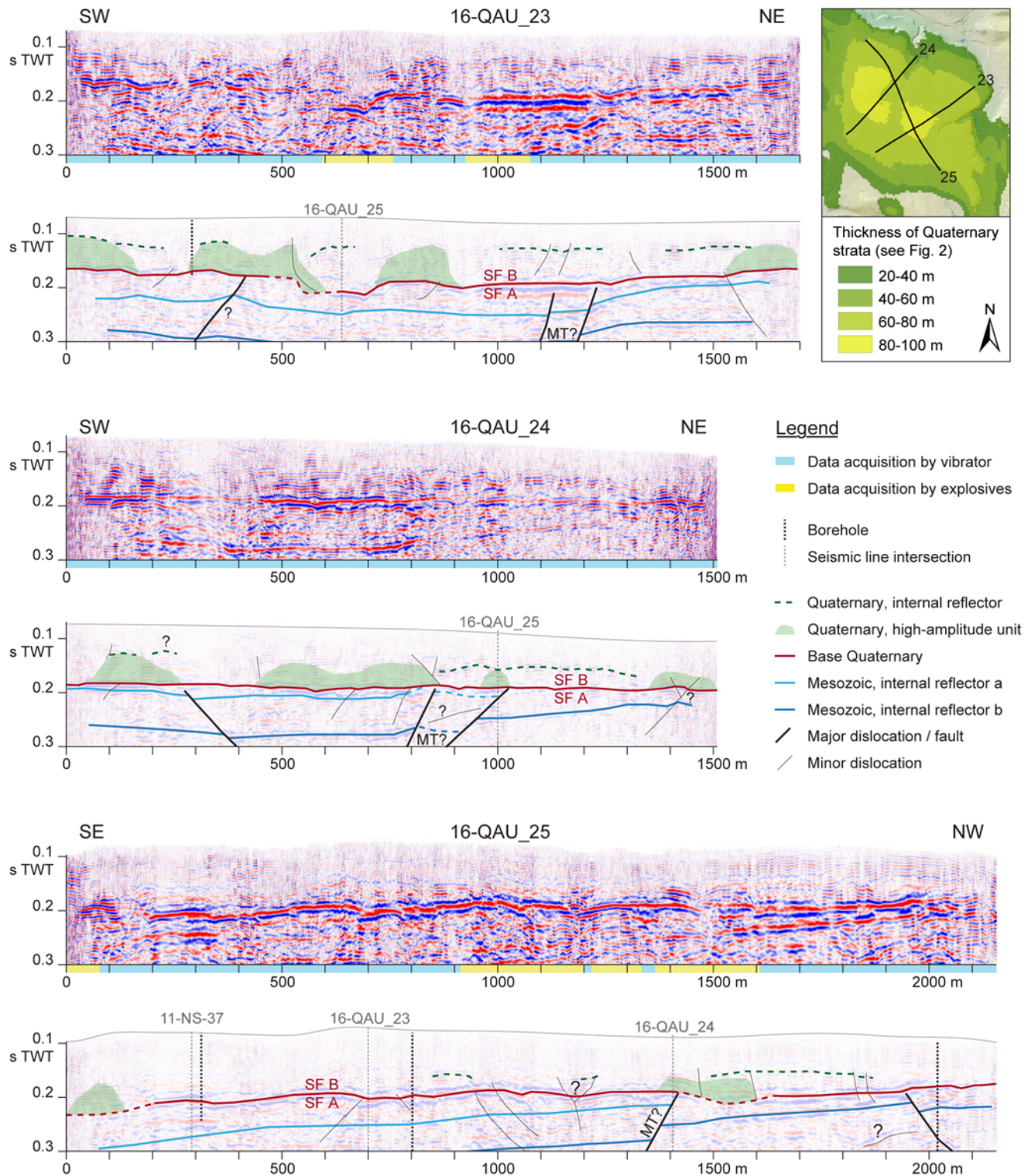


Figure 9. Seismic sections 16_QAU-23, 16_QAU-24, and 16_QAU-25 with interpretation. SF = seismic facies, MT = Mandach Thrust (see Figure 2), seismic line 11-NS-37 from Madritsch *et al.*, 2013. Within the Quaternary, 0.1 s two-way travel time (TWT) corresponds to ~65 m depth (Jäckli, 2012).

would have to be the case to explain the amounts of Alpine limestones (considered freshly delivered material; cf., Schlüchter, 1975) in some samples that are larger than the Limmat reference samples (Fig. 8). The deposits might represent different phases (e.g., advance or retreat) during a glacial cycle, where erosion rates, and

potentially their spatial pattern, can vary significantly (cf., Koppes *et al.*, 2010; Aitken *et al.*, 2016).

In summary, we observe clear evidence for two separate glaciofluvial gravel units in the HRPC, the older (Habsburg Gravel) deposited on top of a subglacial till bed, whereas the younger

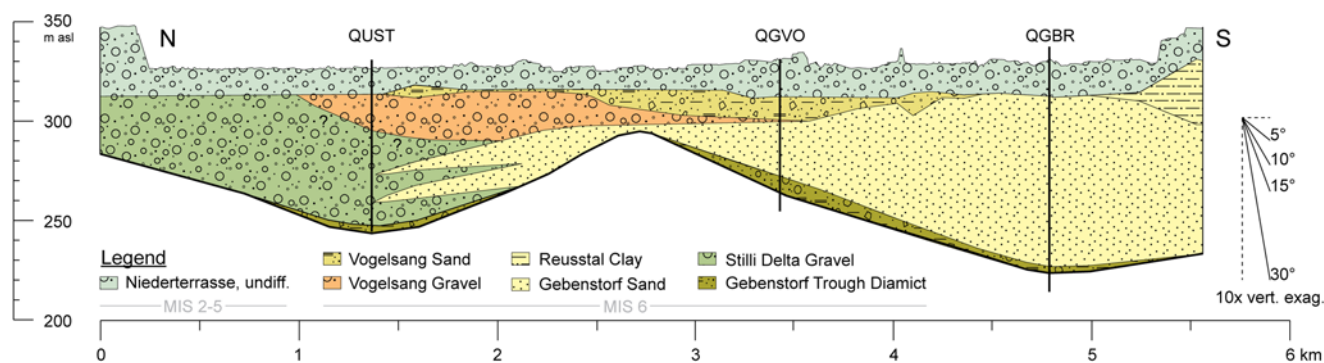


Figure 10. Longitudinal section A (from Gegg et al., 2021, altered; see Figure 2 for location) along the GST. Profile B (Figure 11) intersects at ~4 km.

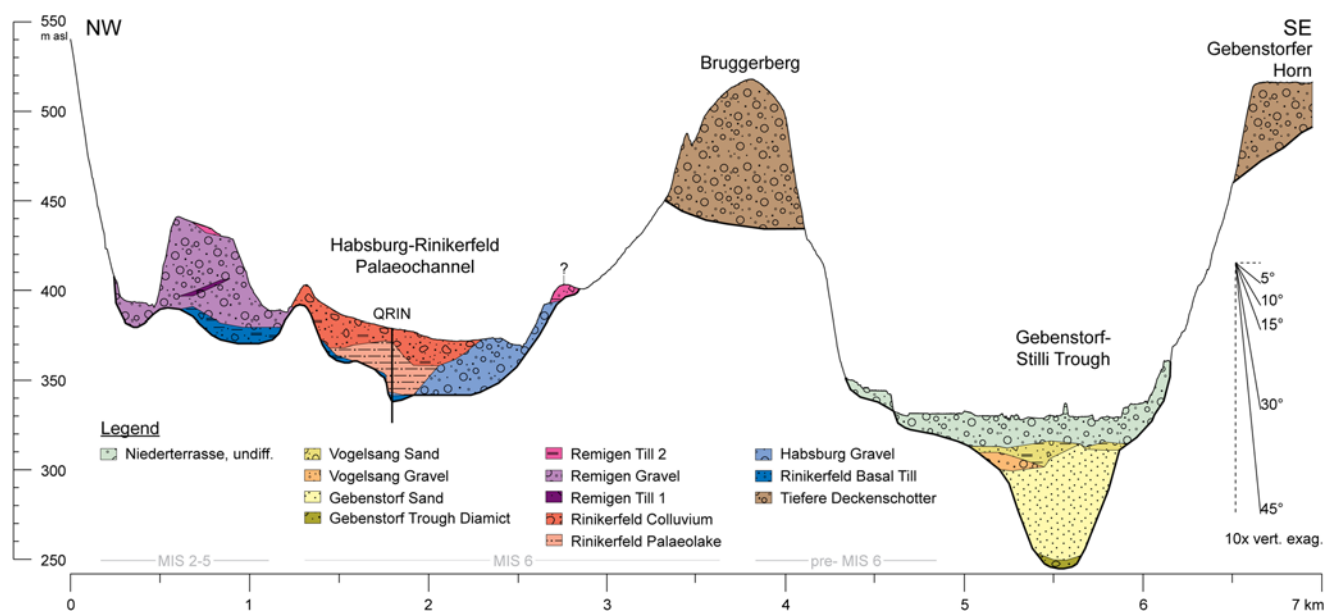


Figure 11. Cross-section B (see Figure 2 for location) through the study area illustrating the stratigraphy of the HRPC (see Gegg et al., 2023) and the overdeepened GST. Profile A (Figure 10) intersects at ~5.5 km.

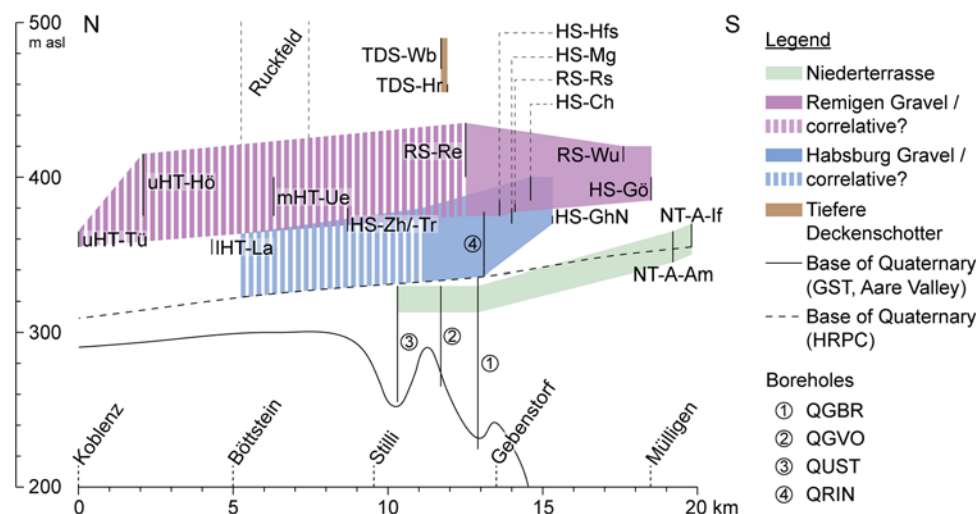


Figure 12. Schematic longitudinal profile through the study area, from the JFTB in the south (right) to the High Rhine in the north (left; see Figure 2). Polygons represent the positions of the different glaciofluvial units, labels refer to outcrops as listed in Supplementary Table 1. Base of Quaternary from Pietsch and Jordan (2014) and Gegg et al. (2021).

(Remigen Gravel) contains intercalated till and/or a till cover at a few locations (Fig. 11). The stratigraphic architecture of the Ruckfeld few km farther downstream (Fig. 2) fits seamlessly into this pattern. In concert with regional-scale seismic data, we interpret SF A as Mesozoic strata that, north of the JFTB, occur in a largely undisturbed, subhorizontal pattern (Fig. 9; major internal reflections a and b of the Mesozoic likely represent the base of the Upper Jurassic Wildegge Formation and Middle Jurassic Klingnau Formation, respectively; cf., Madritsch et al., 2013). SF B represents Quaternary strata that unconformably overlie the Mesozoic bedrock at ca. 0.2 s TWT. The base of the Quaternary is slightly irregular but shows no evidence of overdeepening (cf., Graf, 2009a); the largest depression at ~600 m along line 16-QUAU_23 is likely an incised fluvial channel.

In some places, a horizontal internal reflection separates the Pleistocene into a lower and an upper part. The lower part contains distinct units of higher-amplitude irregular reflectors that are filled in with largely seismically transparent material. We interpret the former as till bodies (i.e., moraine ridges or a dissected ice-decay landscape) covered by glaciofluvial outwash. Comparable seismic facies are connected to similar lithologies for example in the Tannwald Basin in southwestern Germany (~100 km ENE; Burschil et al., 2018, SF A; Schuster et al., 2024). Some minor dislocations can be observed, often adjacent to the presumed till bodies, and thus are considered a result of sagging after melting of dead ice, or of later glaciotectionic deformation. We further suggest correlation of the lower subunit with the Habsburg Gravel and underlying till, and correlation of the upper, mostly transparent subunit with the Remigen Gravel of the HRPC (with a more or less extensive loess cover; Preusser and Graf, 2002; Fig. 12), supporting a two-phase aggrading origin of the Ruckfeld gravel plain, as suggested by Bitterli et al. (2000). It is noteworthy that the Ruckfeld is located directly above the northernmost thrust of the JFTB (Mandach Thrust; Fig. 2; Bitterli-Brunner, 1987; Madritsch et al., 2024). While some indications of Early Pleistocene activity have been reported (Graf, 1993; Bitterli et al., 2000), no clear dislocation of the Middle Pleistocene glaciofluvial deposits of the Ruckfeld along this fault can be identified.

Chronology

A tentative sequence of glacial advances and geomorphic events across the study area was proposed by Bitterli-Dreher et al. (2007) and Graf (2009a). It is here compared with results from this study together with luminescence age estimates by Mueller et al. (2020, 2024) as well as detailed investigations of the QRIN profile by Gegg et al. (2023). Previously, it was suggested that the HRPC was formed prior to, and occupied by glacier ice during, the Möhlin Glacial ('most extensive glaciation'), which likely represents MIS 12 (Preusser et al., 2021; Dieleman et al., 2022b). The paleolake deposits in the Rinikerfeld have been tentatively attributed to the retreat phase of this glaciation. Two later proposed ice advances of lesser extent, termed Habsburg and Hagenholz (MIS 10–8?), resulted mainly in the accumulation of glaciofluvial gravels along the HRPC and its northward continuation. These are Habsburg Gravel and Upper Hochterrasse, and Ruckfeld Gravel and Middle Hochterrasse, respectively (Bitterli-Dreher et al., 2007; Graf, 2009a). The Rinikerfeld Basal Till from QRIN thus represents the first documented phase of glacial occupancy in the HRPC, and our gravel petrographic data indicate that it was deposited by the same glacier, and thus during the same glaciation, as the Habsburg Gravel (Figs. 7 and 8; Gegg et al., 2023). Unfortunately,

no sand layers or lenses suitable for luminescence dating were encountered in either QRIN or one of the outcrops of the Habsburg Gravel. We consider it not unlikely that these deposits represent the Möhlin Glacial/MIS 12 (e.g., Graf, 2009a), but also a later phase (Habsburg/MIS 10?; e.g., Preusser et al., 2011) cannot be excluded (Figs. 1, 13A, B). The Rinikerfeld Paleolake however is clearly younger (see below).

The Beringen Glacial (MIS 6) reached far north into the High Rhine Valley and reflects the last phase of glaciofluvial drainage through the HRPC, before development of the current Wasserschloss (Bitterli-Dreher et al., 2007; Graf, 2009a; Preusser et al., 2011). The paleolake deposits in the Rinikerfeld recently have been shown to reflect a phase of ice retreat during early MIS 6 (Fig. 13C; Mueller et al., 2020, 2024; Gegg et al., 2023). Mueller et al. (2024) provided minimum depositional ages corresponding to MIS 5 for outcrops of the Remigen Gravel (HABS = Götschtel gravel pit/outcrop 5, $> 100 \pm 12$ ka; RINI = Alpberg gravel pit/outcrop 10, $> 92 \pm 13$ ka; see Fig. 2 and Supplementary Table 2). We suggest that deposition of the Remigen Gravel may have started during the same early MIS 6 ice advance (~Hagenholz sensu Keller and Krayss, 2010) and continued with the following second MIS 6 ice advance (in agreement with Bitterli-Dreher et al., 2007; Graf, 2009a; Preusser et al., 2011). Both the Rinikerfeld Paleolake as well as the Remigen Gravel (and the proposed correlative deposits of the Ruckfeld and Upper Hochterrasse) show good evidence of being overridden by a later ice advance despite their position well outside the maximum Late Pleistocene glacier extent (e.g., Preusser et al., 2011). A similar situation in the form of an early ice advance followed by a phase of glaciofluvial or glaciolacustrine deposition and a second, extensive ice advance later during the same glacial period was suggested for overdeepening-fill profiles in the Wehntal (Anselmetti et al., 2010; Dehnert et al., 2012) and Lower Glatt Valley (Buechi et al., 2018), both also dated to MIS 6. This vast second Beringen advance marks the last phase of glacial (or glaciofluvial) occupancy in the HRPC (Fig. 13D).

While the initial formation of the overdeepened Birrfeld Basin (Fig. 2) probably started during the Habsburg Glacial at the latest, incision of the GST is also attributed to the Beringen Glacial. It has been argued that formation of the GST would have caused abandonment of the HRPC (Bitterli-Dreher et al., 2007; Graf, 2009a; Gegg et al., 2023). MIS 5 minimum ages have been reported for the glaciolacustrine/glaciodeltaic infill of the GST at QGBR (91.6 m depth; $> 92 \pm 22$ ka) and QUST (33.2 m depth, $> 104 \pm 14$ ka) in Mueller et al. (2024). An incision during the second Beringen advance is indeed the most likely scenario for formation of the GST. This was followed by its infilling with sediments upon the beginning of ice decay as well as re-adjustment of the local drainage network (Fig. 13E). A second inlaid basin within the GST (Fig. 10) finally attests to a third Beringen ice advance into the study area (Fig. 13F). This complex sequence of events agrees with luminescence data from the Klettgau area (Lowick et al., 2015) that indicate up to four phases of deposition along the High Rhine during MIS 6.

The last glacial cycle, regionally referred to as Birrfeld Glacial, spans the majority of the Late Pleistocene (Preusser, 2004; Ivy-Ochs et al., 2008) and, in our study area, is represented by glaciofluvial Niederterrasse gravel along the current river valleys. It comprises three phases of ice build-up in the Central Alps, with the final one peaking at ca. 25 ka (MIS 2; Gaar et al., 2019; Kamleitner et al., 2023). Gaar et al. (2019) present luminescence ages from Niederterrasse deposits in the Aare Valley and Birrfeld/Reuss Valley that correspond to this regional last glacial maximum.

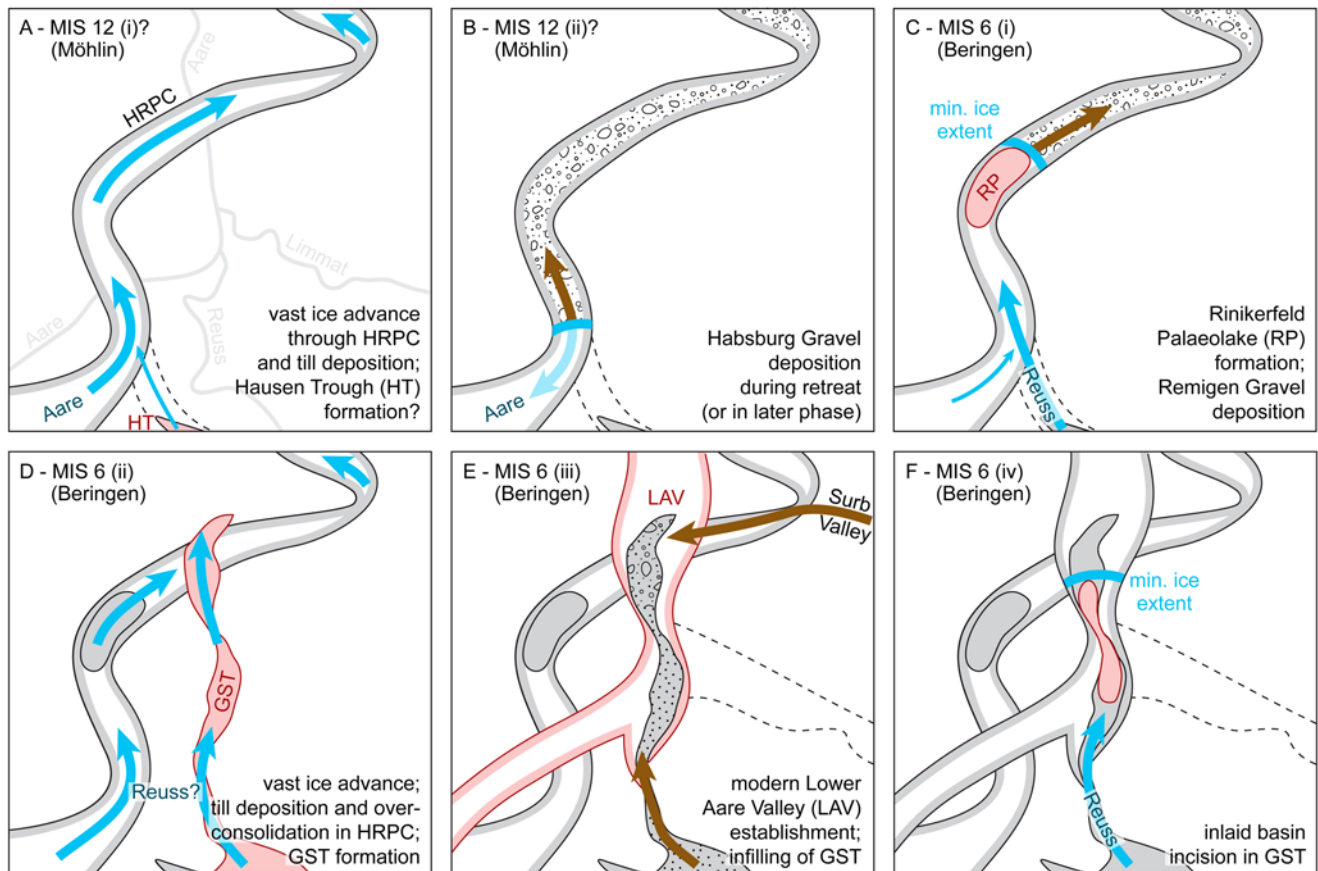


Figure 13. Schematic sketch of the Wasserschloss area's proposed evolution during the Middle Pleistocene. (A) Advance by a paleo-Aare glacier along the HRPC, possibly in MIS 12 (Möhlín Glacial/'most extensive glaciation') left a sporadic basal till layer behind. Present-day rivers are plotted in light gray for orientation (see Figure 2). (B) The Habsburg Gravel was deposited either by the same glacier during its retreat (brown arrow) or, alternatively, in a later glaciation such as MIS 10. (C) Advance of a paleo-Reuss glacier into the HRPC in early MIS 6 (Beringen Glacial) resulted in lake formation in the Rinikerfeld and deposition of the Remigen Gravel. (D) Later during the same glaciation, an extensive ice advance overrode the study area, leading to overconsolidation of the Rinikerfeld Palaeolake, till deposition on top of the Remigen Gravel, and likely incision of the GST. (E) Infilling of the GST started with onset of glacier retreat. With the GST established, drainage was significantly lowered (~50 m below the HRPC) and rerouted. The modern Limmat Valley (dashed) was probably not active as gravel of Limmat provenance was being delivered into the GST via the Surb Valley (Graf, 2009a). (F) An inlaid overdeepened basin attests to the re-advancement of a paleo-Reuss glacier over the GST.

Cosmogenic nuclide data from moraines in the same area (Reber et al., 2014) as well as radiocarbon data of mammoth tusks and other macrofossils found in several gravel pits (Graf, 2009a) yield similar ages.

In contrast, luminescence dating of two Niederterrasse samples from QGBR (11.2 m depth, ca. 90 ka) and QUST (13.2 m depth, > ca. 50 ka) by Mueller et al. (2024) resulted in ages corresponding to late MIS 5 and MIS 3 or earlier, respectively. This is perhaps unexpected but not unrealistic, because two earlier Late Pleistocene ice advances occurred during MIS 5d and MIS 4 (Fig. 1; Ivy-Ochs et al., 2008; Preusser et al., 2011). Glaciofluvial outwash corresponding to a cold phase in MIS 5d was previously identified farther upstream in the Aare Valley (Thalgut; Preusser and Schlüchter, 2004), in the Glatt (Gossau; Preusser et al., 2003) and Klettgau valleys (Lowick et al., 2015), and potentially also in the Reuss Valley (Gaar et al., 2019). MIS 4 deposits are known from the Rhone piedmont glacier area (Preusser et al., 2007) and in the Reuss Valley in close vicinity to our study area (Preusser and Graf, 2002; Gaar et al., 2019). The occurrence of the same older Upper Pleistocene gravels in the Wasserschloss area, in shallow depth and close to the present-day river course, emphasizes that the corresponding ice advances produced considerable amounts of sediment. However, reworking of

MIS 5d- or MIS 4-aged gravels without sufficient light exposure to reset the luminescence signal during MIS 2 cannot be excluded.

Conclusions

We presented results from an extensive drilling and field campaign targeted at the (Middle) Pleistocene sedimentary archives in the Wasserschloss area, the confluence of the Aare, Reuss, and Limmat rivers in Northern Switzerland. These archives occur in the Habsburg-Rinikerfeld Palaeochannel (HRPC), which is part of a now elevated, older drainage network that is only sporadically preserved, and in the overdeepened Gebenstorf-Stilli Trough (GST) that underlies the current river path. In the HRPC an early Middle Pleistocene occupancy by a glacier with a dominant Aare signature in its deposits, potentially during MIS 12, is recorded by basal till and glaciofluvial outwash. In a later phase, most likely during MIS 6, another glacier advanced into the HRPC twice, leaving behind sporadic occurrences of lake deposits, till, and large amounts of glaciofluvial gravel with a dominant Reuss signature. Presumably during the extensive second advance, subglacial erosion sculpted the GST, a new pathway that was subsequently infilled by thick glaciodeltaic to glaciolacustrine sands and gravels.

These were finally overridden and partly re-excavated by a third MIS 6 ice advance. This complex pattern of at least two separate ice advances appears to be characteristic of the penultimate glaciation in the midlands of Northern Switzerland and beyond. The incision of the GST triggered local re-arrangement of the river system, with abandonment of the HRPC and development of the modern Wasserschloss morphology. In the Late Pleistocene, glaciofluvial gravels were deposited along the modern river valleys in three distinct phases (MIS 5d, MIS 4, and MIS 2).

The study area stands out from the majority of other Quaternary sites in the Swiss Alpine foreland due to its local geological and topographic settings. While many well-studied localities are situated in the Molasse Basin, the GST and HRPC lie within the easternmost Jura Mountains. In these diverse but generally rather erosion-resistant Mesozoic rocks, pronounced relief developed with morphologically well-defined and comparatively stable valleys. As a result, the Pleistocene ice advances and meltwater streams were not only topographically constrained but also repeatedly directed along the same pathways. One consequence of the repeated occupation of the same valleys is a complex, interwoven stratigraphy whose components are difficult to identify and resolve. This study emphasizes the potential of gravel petrographic analyses that can help distinguish genetic units and build a relative stratigraphy even where chronostratigraphic approaches are difficult. A second consequence is a preservation potential for glacial deposits (*sensu lato*) that locally is even smaller than in other areas, as multiple phases of glacial and/or glaciofluvial reactivation of the same valleys effectively obliterate older remnants. Consequently, we encountered mainly sediments that we attribute to the regionally extensive penultimate glaciation (Beringen Glacial, MIS 6), although some relicts presumably represent an older stage that might be the 'most extensive glaciation' (Möhlin Glacial, likely MIS 12). We suggest that the regional and over-regional Quaternary record can still be further expanded, and the landscape history better understood by detailed sedimentological and petrographic analyses combined with state-of-the-art geochronology.

Supplementary material. The supplementary material for this article can be found at <https://doi.org/10.1017/qua.2024.61>.

Acknowledgments. This study was facilitated by the Swiss National Cooperative for the Disposal of Radioactive Waste (Nagra). We would also like to kindly thank Hansruedi Graf, Angela Landgraf, Hendrik Vogel for valuable input and recommendations, and Julijana Gajic for performing the geochemical analyses. We thank Dominik Amschwand, Marius Huber, Andrea Kuster, Kim Lemke, Dominik Schmid, and Stephanie Talker for support during field and laboratory work. The initial manuscript benefitted from constructive recommendations by Laura Stutenbecker, an anonymous reviewer, as well as editor Nicholas Lancaster.

Competing interests. The authors declare none.

References

- Aitken, A.R.A., Roberts, J.L., Ommen, T.V., Young, D.A., Golledge, N.R., Greenbaum, J.S., Blankenship, D.D., Siegert, M.J., 2016. Repeated large-scale retreat and advance of Totten Glacier indicated by inland bed erosion. *Nature* 533, 385–389.
- Akçar, N., Ivy-Ochs, S., Alfimov, V., Schlunegger, F., Claude, A., Reber, R., Christl, M., et al., 2017. Isochron-burial dating of glaciofluvial deposits: first results from the Swiss Alps. *Earth Surface Processes And Landforms* 42, 2414–2425.
- Alley, R.B., Cuffey, K.M., Evenson, E.B., Strasser, J.C., Lawson, D.E., Larson, G.J., 1997. How glaciers entrain and transport basal sediment: physical constraints. *Quaternary Science Reviews* 16, 1017–1038.
- Alley, R.B., Cuffey, K.M., Zoet, L.K., 2019. Glacial erosion: status and outlook. *Annals of Glaciology* 60, 1–13.
- Anselmetti, F.S., Drescher-Schneider, R., Furrer, H., Graf, H.R., Lowick, S.E., Preusser, F., Riedi, M.A., 2010. A ~180,000 years sedimentation history of a perialpine overdeepened glacial trough (Wehntal, N-Switzerland). *Swiss Journal of Geosciences* 103, 345–361.
- Berger, J.-P., Reichenbacher, B., Becker, D., Grimm, M., Grimm, K., Picot, L., Storni, A., Pirkenseer, C., Derer, C., Schaefer, A., 2005. Palaeogeography of the upper Rhine Graben (URG) and the Swiss Molasse basin (SMB) from Eocene to Pliocene. *International Journal of Earth Sciences* 94, 697–710.
- Bini, A., Buoncristiani, J.F., Couterrand, S., Ellwanger, D., Felber, M., Florineth, D., Graf, H.R., Keller, O., Kelly, M., Schlüchter, C., 2009. *Die Schweiz Während des Letztzeiszeitlichen Maximums (LGM) 1:500.000*. Federal Office of Topography Swisstopo, Wabern.
- Bitterli, T., Graf, H.R., Matousek, F., Wanner, M., 2000. *Geologischer Atlas der Schweiz 1:25.000. Blatt 1050 Zurzach. Erläuterungen*. Federal Office of Topography Swisstopo, Wabern.
- Bitterli-Brunner, P., 1987. Die Mandacher und Mettauer Aufschiebungen (Aargauer Tafeljura) aufgrund neuer Untersuchungen. *Bulletin der Vereinigung der Schweizerischen Petroleumgeologen und Petroleumingenieure* 53, 23–26.
- Bitterli-Dreher, P., Graf, H.R., Naef, H., Diebold, P., Matousek, F., Burger, H., Pauli-Gabi, T., 2007. *Geologischer Atlas der Schweiz 1:25.000. Blatt 1070 Baden. Erläuterungen*. Federal Office of Topography Swisstopo, Wabern.
- Boulton, G.S., Paul, M.A., 1976. The influence of genetic processes on some geotechnical properties of glacial tills. *Quarterly Journal of Engineering Geology* 9, 159–194.
- Boyle, J.F., 2001. Inorganic geochemical methods in palaeolimnology. In: Last, W.M., Smol, J.P. (Eds.) *Tracking Environmental Change Using Lake Sediments. Developments in Paleoenvironmental Research* 2. Springer, Dordrecht. https://doi.org/10.1007/0-306-47670-3_5
- Buechi, M.W., Graf, H.R., Haldimann, P., Lowick, S.E., Anselmetti, F.S., 2018. Multiple Quaternary erosion and infill cycles in overdeepened basins of the northern Alpine foreland. *Swiss Journal of Geosciences* 111, 133–167.
- Buechi, M.W., Landgraf, A., Madritsch, H., Mueller, D., Knipping, M., Nyffenegger, F., Preusser, F., Schaller, S., Schnellmann, M., Deplazes, G., 2024. Terminal glacial overdeepenings: patterns of erosion, infilling and new constraints on the glaciation history of Northern Switzerland. *Quaternary Science Reviews* 344, 108970. <https://doi.org/10.1016/j.quascirev.2024.108970>
- Bugmann, E., 1961. Beiträge zur Gliederung der Risszeitlichen Bildungen in der Nordschweiz. *Mitteilungen der Aargauischen Naturforschenden Gesellschaft* 26, 105–119.
- Burkhard, M., 1990. Aspects of the large-scale Miocene deformation in the most external part of the Swiss Alps (sub-Alpine molasse to Jura fold belt). *Eclogae Geologicae Helveticae* 83, 559–583.
- Burkhard, M., Sommaruga, A., 1998. Evolution of the western Swiss Molasse basin: structural relations with the Alps and the Jura belt. *Geological Society, London, Special Publications* 134, 279–298.
- Burschil, T., Bunes, H., Tanner, D.C., Wielandt-Schuster, U., Ellwanger, D., Gabriel, G., 2018. High-resolution reflection seismics reveal the structure and the evolution of the Quaternary glacial Tannwald Basin. *Near Surface Geophysics* 16, 593–610.
- Chiverrell, R.C., Smedley, R.K., Small, D., Ballantyne, C.K., Burke, M.J., Callard, S.L., Clark, C.D., Duiller, G.A.T., Evans, D.J.A., Fabel, D., 2018. Ice margin oscillations during deglaciation of the northern Irish Sea Basin. *Journal of Quaternary Science* 33, 739–762.
- Claude, A., Akçar, N., Ivy-Ochs, S., Schlunegger, F., Rentzel, P., Pümpin, C., Tikhomirov, D., Kubik, P.W., Vockenhuber, C., Dehnert, A., 2017. Chronology of Quaternary terrace deposits at the locality Hohle Gasse (Pratteln, NW Switzerland). *Swiss Journal of Geosciences* 110, 793–809.
- Cook, S.J., Swift, D.A., 2012. Subglacial basins: their origin and importance in glacial systems and landscapes. *Earth-Science Reviews* 115, 332–372.
- Dehnert, A., Lowick, S.E., Preusser, F., Anselmetti, F.S., Drescher-Schneider, R., Graf, H.R., Heller, F., Horstmeyer, H., Kemna, H.A., Nowaczyk, N.R., 2012. Evolution of an overdeepened trough in the northern Alpine Foreland at Niederweningen, Switzerland. *Quaternary Science Reviews* 34, 127–145.

- Den Brok, B., Caduff, R., Kempf, O., 2021. *Geologischer Atlas der Schweiz 1:25.000. Blatt 1174 Elm. Erläuterungen*. Federal Office of Topography Swisstopo, Wabern.
- Dick, K.A., Graf, H.R., Müller, B.U., Hartmann, P., Schlüchter, C., 1996. Das nordalpine Wasserschloss und seine eiszeitgeologische Umgebung. *Eclogae Geologicae Helveticae* **89**, 635–645.
- Dieleman, C., Christl, M., Vockenhuber, C., Gautschi, P., Akçar, N., 2022a. Early Pleistocene complex cut-and-fill sequences in the Alps. *Swiss Journal of Geosciences* **115**, 11. <https://doi.org/10.1186/s00015-022-00411-2>
- Dieleman, C., Christl, M., Vockenhuber, C., Gautschi, P., Graf, H.R., Akçar, N., 2022b. Age of the most extensive glaciation in the Alps. *Geosciences* **12**, 39. <https://doi.org/10.3390/geosciences12010039>
- Dietze, E., Dietze, M., 2019. Grain-size distribution unmixing using the R package EMMAgeo. *E&G Quaternary Science Journal* **68**, 29–46.
- Dürst Stucki, M., Schlunegger, F., 2013. Identification of erosional mechanisms during past glaciations based on a bedrock surface model of the central European Alps. *Earth and Planetary Science Letters* **384**, 57–70.
- Ehlers, J., Gibbard, P.L., Hughes, P.D. (Eds.), 2011. *Quaternary Glaciations—Extent and Chronology. Developments in Quaternary Science 15*. Elsevier, Amsterdam, 1126 pp.
- Evans, D.J.A., Phillips, E.R., Hiemstra, J.F., Auton, C.A., 2006. Subglacial till: formation, sedimentary characteristics and classification. *Earth-Science Reviews* **78**, 115–176.
- Eyles, N., Eyles, C.H., Miall, A.D., 1983. Lithofacies types and vertical profile models; an alternative approach to the description and environmental interpretation of glacial diamict and diamictite sequences. *Sedimentology* **30**, 393–410.
- Gaar, D., Graf, H.R., Preusser, F., 2019. New chronological constraints on the timing of Late Pleistocene glacier advances in Northern Switzerland. *E&G Quaternary Science Journal* **68**, 53–73.
- Gegg, L., Anselmetti, F.S., Deplazes, G., Knipping, M., Madritsch, H., Mueller, D., Preusser, F., Vogel, H., Buechi, M.W., 2023. Rinikerfeld Palaeolake (Northern Switzerland)—a sedimentary archive of landscape and climate change during the penultimate glacial cycle. *Journal of Quaternary Science* **38**, 174–185.
- Gegg, L., Buechi, M.W., Ebert, A., Deplazes, G., Madritsch, H., Anselmetti, F.S., 2020. Brecciation of glacially overridden palaeokarst (Lower Aare Valley, Northern Switzerland): result of subglacial water-pressure peaks? *Boreas* **49**, 813–827.
- Gegg, L., Deplazes, G., Keller, L., Madritsch, H., Spillmann, T., Anselmetti, F.S., Buechi, M.W., 2021. 3D morphology of a glacially overdeepened trough controlled by underlying bedrock geology. *Geomorphology* **394**, 107950. <https://doi.org/10.1016/j.geomorph.2021.107950>
- Gegg, L., Griebeling, F., Jentz, N., Wielandt-Schuster, U., 2024. Towards a quantitative lithostratigraphy of Pleistocene fluvial deposits in the southern Upper Rhine Graben. *E&G Quaternary Science Journal* **73**, 239–249.
- Gegg, L., Kuster, A.M., Amschwand, D., Huber, M., Deplazes, G., Madritsch, H., Buechi, M.W., 2019b. *Quaternary Borehole QBO Gebenstorf-Vogelsang (QVGO) Data Report*. Nagra Arbeitsbericht NAB 19-03. <https://nagra.ch/en/downloads/arbeitsbericht-nab-19-03-2>
- Gegg, L., Kuster, A.M., Deplazes, G., Madritsch, H., Buechi, M.W., 2019a. *Quaternary Borehole QBO Gebenstorf-Brüel (QGBR) Data Report*. Nagra Arbeitsbericht NAB 19-02. <https://nagra.ch/en/downloads/arbeitsbericht-nab-19-02-2>
- Gegg, L., Kuster, A.M., Schmid, D., Buechi, M.W., 2018. *Quaternary Boreholes QBO Riniken-1 and -2 (QRIN1 and QRIN2) Data Report*. Nagra Arbeitsbericht NAB 18-40. <https://nagra.ch/en/downloads/arbeitsbericht-nab-18-40-2>
- Gegg, L., Kuster, A.M., Schmid, D., Lemke, K., Deplazes, G., Madritsch, H., Buechi, M.W., 2019c. *Quaternary Borehole QBO Untersiggenthal (QUST) Data Report*. Nagra Arbeitsbericht NAB 19-01. <https://nagra.ch/en/downloads/arbeitsbericht-nab-19-01-2>
- Gegg, L., Preusser, F., 2023. Comparison of overdeepened structures in formerly glaciated areas of the northern Alpine foreland and northern central Europe. *E&G Quaternary Science Journal* **72**, 23–36.
- Gilbert, G.L., Cable, S., Thiel, C., Christiansen, H.H., Elberling, B., 2017. Cryostratigraphy, sedimentology, and the late Quaternary evolution of the Zackenberg River delta, northeast Greenland. *The Cryosphere* **11**, 1265–1282.
- Graf, A., Akçar, N., Ivy-Ochs, S., Strasky, S., Kubik, P.W., Christl, M., Burkhard, M., Wieler, R., Schlüchter, C., 2015. Multiple advances of Alpine glaciers into the Jura Mountains in the Northwestern Switzerland. *Swiss Journal of Geosciences* **108**, 225–238.
- Graf, H.R., 1993. Die Deckenschotter der zentralen Nordschweiz. Ph.D. Thesis, ETH Zurich, Switzerland. <https://www.research-collection.ethz.ch/handle/20.500.11850/141237>
- Graf, H.R., 2009a. *Stratigraphie von Mittel- und Spätpleistozän in der Nordschweiz, Beiträge zur Geologischen Karte der Schweiz N. F. 168*. Federal Office of Topography Swisstopo, Wabern.
- Graf, H.R., 2009b. Stratigraphie und Morphogenese von frühpleistozänen Ablagerungen zwischen Bodensee und Klettgau. *Quaternary Science Journal* **58**, 12–53.
- Graf, H.R., Bitterli-Dreher, P., Burger, H., Bitterli, T., Diebold, P., Naef, H., 2006. *Geologischer Atlas der Schweiz 1:25.000, Blatt 1070 Baden*. Federal Office of Topography Swisstopo, Wabern.
- Graf, H.R., Burkhalter, R., 2016. Quaternary deposits: concept for a stratigraphic classification and nomenclature—an example from Northern Switzerland. *Swiss Journal of Geosciences* **109**, 137–147.
- Hammer, Ø., Harper, D.A.T., Ryan, P.D., 2001. PAST: paleontological statistics software package for education and data analysis. *Palaeontologia Electronica* **4**, 9. http://palaeo-electronica.org/2001_1/past/issue1_01.htm
- Hantke, R., 1978. *Eiszeitalter. Die jüngste Erdgeschichte der Schweiz und ihrer Nachbargebiete. Band 1—Klima, Flora, Fauna, Mensch, Alt- und Mittel-Pleistozän, Vogesen, Schwarzwald, Schwäbische Alb, Adelegg*. Ott Verlag, Thun, Switzerland.
- Hantke, R., Brückner, W., 2011. *Geologischer Atlas der Schweiz 1:25.000. Blatt 1192 Schächental. Erläuterungen*. Federal Office of Topography Swisstopo, Wabern.
- Hughes, P.D., Gibbard, P.L., Ehlers, J., 2019. The “missing glaciations” of the Middle Pleistocene. *Quaternary Research* **96**, 161–183.
- Ivy-Ochs, S., Kerschner, H., Reuther, A., Preusser, F., Heine, K., Maisch, M., Kubik, P.W., Schlüchter, C., 2008. Chronology of the last glacial cycle in the European Alps. *Journal of Quaternary Science* **23**, 559–573.
- Jäckli, H., 2012. *2D-Seismik Nordschweiz 2011/12: Geologische Aufnahme der Aufzeitbohrungen (Teil 1) und Aufzeitmessungen (Teil 2)*. Nagra Arbeitsbericht NAB 12-22. <https://nagra.ch/downloads/arbeitsbericht-nab-12-22>
- Jordan, P., 2010. Analysis of overdeepened valleys using the digital elevation model of the bedrock surface of Northern Switzerland. *Swiss Journal of Geosciences* **103**, 375–384.
- Jordan, P., Wetzel, A., Reisdorf, A., 2008. Swiss Jura Mountains. In: McCann, T. (Ed.), *The Geology of Central Europe*. Geological Society of London, London, pp. 823–923.
- Kamleitner, S., Ivy-Ochs, S., Manatschal, L., Akçar, N., Christl, M., Vockenhuber, C., Hajdas, I., Synal, H.A., 2023. Last glacial maximum glacier fluctuations on the northern Alpine foreland: geomorphological and chronological reconstructions from the Rhine and Reuss glacier systems. *Geomorphology* **423**, 108548. <https://doi.org/10.1016/j.geomorph.2022.108548>
- Keller, O., Kravay, E., 2010. Mittel- und spätpleistozäne stratigraphie und morphogenese in Schlüsselregionen der Nordschweiz. *E&G Quaternary Science Journal* **59**, 88–119.
- Koppes, M., Sylwester, R., Rivera, A., Hallet, B., 2010. Variations in sediment yield over the advance and retreat of a calving glacier, Laguna San Rafael, North Patagonian Icefield. *Quaternary Research* **73**, 84–95.
- Krotz, O., Giazzi, G., 2018. *Elemental Analysis: CHNS/O Determination of Marine Samples*. ThermoFisher Scientific, Application Note, AN42304-EN 0618. <https://assets.thermofisher.com/TFS-Assets/CMD/Application-Notes/an-42304-oca-chsno-marine-science-an42304-en.pdf>
- Kuhlemann, J., Rahn, M., 2013. Plio-Pleistocene landscape evolution in Northern Switzerland. *Swiss Journal of Geosciences* **106**, 451–467.

- Leonard, E.M., 1986. Varve studies at Hector Lake, Alberta, Canada, and the relationship between glacial activity and sedimentation. *Quaternary Research* **25**, 199–214.
- Lisiecki, L.E., Raymo, M.E., 2005. A Pliocene–Pleistocene stack of 57 globally distributed benthic $\delta^{18}\text{O}$ records. *Paleoceanography* **20**, PA1003. <https://doi.org/10.1029/2004PA001071>
- Looser, N., Madritsch, H., Guillong, M., Laurent, O., Wohlwend, S., Bernasconi, S.M., 2021. Absolute age and temperature constraints on deformation along the basal décollement of the Jura Fold-and-thrust Belt from carbonate U–Pb dating and clumped isotopes. *Tectonics* **40**, e2020TC006439. <https://doi.org/10.1029/2020TC006439>
- Lowick, S.E., Buechi, M.W., Gaar, D., Graf, H.R., Preusser, F., 2015. Luminescence dating of Middle Pleistocene proglacial deposits from Northern Switzerland: methodological aspects and stratigraphical conclusions. *Boreas* **44**, 459–482.
- Lu, G., Winkler, W., Rahn, M., von Quadt, R., Willet, S.D., 2018. Evaluating igneous sources of the Taveyannaz Formation in the Central Alps by detrital zircon U–Pb age dating and geochemistry. *Swiss Journal of Geosciences* **111**, 399–416.
- Madritsch, H., Looser, N., Schneeberger, S., Wohlwend, S., Guillong, M., Malz, A., 2024. Reconstructing the evolution of foreland fold-and-thrust belts using U–Pb calcite dating: an integrated case-study from the eastern-most Jura Mountains (Switzerland). *Tectonics* **43**, e2023TC008181. <https://doi.org/10.1029/2023TC008181>
- Madritsch, H., Meier, B., Kuhn, P., Roth, P., Zingg, O., Heuberger, S., Naef, H., Birkhäuser, P., 2013. Regionale Strukturgeologische Zeitinterpretation der Nagra 2D-Seismik 2011/12. Nagra Arbeitsbericht NAB 13-10. <https://nagra.ch/en/downloads/arbeitsbericht-nab-13-10/>
- Matousek, F., Wanner, M., Baumann, A., Graf, H.R., Nüesch, R., Bitterli, T., 2000. *Geologischer Atlas der Schweiz 1:25.000. Blatt 102 Zurzach*. Bundesamt für Landestopografie Swisstopo, Wabern.
- Merritt, J.W., Gordon, J.E., Connell, E.R., 2019. Late Pleistocene sediments, landforms and events in Scotland: a review of the terrestrial stratigraphic record. *Earth and Environmental Science Transactions of the Royal Society of Edinburgh* **110**, 39–91.
- Meyers, P.A., Teranes, J.L., 2001. Sediment organic matter. In: Last, W.M., Smol, J.P. (Eds.), *Tracking Environmental Change Using Lake Sediments 2, Physical and Geochemical Methods*. Kluwer Academic Publishers, Dordrecht, pp. 239–270.
- Miall, A.D., 1977. Lithofacies types and vertical profile models in braided river deposits: a summary. In: Miall, A.D. (Ed.), *Fluvial Sedimentology*. Geological Survey of Canada Memoir 5, pp. 597–604.
- Mills, P.C., 1983. Genesis and diagnostic value of soft-sediment deformation structures—a review. *Sedimentary Geology* **35**, 83–104.
- Mueller, D., Gegg, L., Fülling, A., Buechi, M.W., Deplazes, G., Preusser, F., 2024. Luminescence dating of glaciogenic deposits from Northern Switzerland: comparing small aliquots and single grains. *Quaternary Geochronology* **82**, 101551. <https://doi.org/10.1016/j.quageo.2024.101551>
- Mueller, D., Preusser, F., Buechi, M.W., Gegg, L., Deplazes, G., 2020. Luminescence properties and dating of glacial to periglacial sediments from Northern Switzerland. *Geochronology* **2**, 305–323.
- Mullins, H.T., Hinchey, E.J., 1989. Erosion and infill of New York Finger Lakes: implications for Laurentide ice sheet deglaciation. *Geology* **17**, 622–625.
- Nitsche, F.O., Monin, G., Marillier, F., Graf, H., Anson, J., 2001. Reflection seismic study of Cenozoic sediments in an overdeepened valley of Northern Switzerland: the Birrfeld area. *Eclogae Geologicae Helveticae* **94**, 363–371.
- Peach, P.A., Perrie, L.A., 1975. Grain-size distribution within glacial varves. *Geology* **3**, 43–46.
- Pfander, J., Schlunegger, F., Serra, E., Gribenski, N., Garefalakis, P., Akçar, N., 2022. Glaciofluvial sequences recording the Birrfeld Glaciation (MIS 5d–2) in the Bern area, Swiss Plateau. *Swiss Journal of Geosciences* **115**, 12. <https://doi.org/10.1186/s00015-022-00414-z>
- Pfiffner, O.A., 1986. Evolution of the north Alpine foreland basin in the Central Alps. In: Homewood, P., Allen, P.A. (Eds.), *Foreland Basins. International Association of Sedimentology, Special Publication* **8**, 219–228.
- Pietsch, J., Jordan, P., 2014. *Digitales Höhenmodell Basis Quartär der Nordschweiz – Version 2014 und ausgewählte Auswertungen*. Nagra Arbeitsbericht NAB 14-02. <https://nagra.ch/downloads/arbeitsbericht-nab-14-02>
- Pisarska-Jamroz, M., Weckwerth, P., 2013. Soft-sediment deformation structures in a Pleistocene glaciolacustrine delta and their implications for the recognition of subenvironments in delta deposits. *Sedimentology* **60**, 637–665.
- Pomper, J., Salcher, B.C., Eichkitz, C., Prasicek, G., Lang, A., Lindner, M., Götz, J., 2017. The glacially overdeepened trough of the Salzach Valley, Austria: bedrock geometry and sedimentary fill of a major Alpine subglacial basin. *Geomorphology* **295**, 147–158. <https://doi.org/10.1016/j.geomorph.2017.07.009>
- Preusser, F., 2004. Towards a chronology of the Late Pleistocene in the northern Alpine Foreland. *Boreas* **33**, 195–210.
- Preusser, F., Blei, A., Graf, H., Schlüchter, C., 2007. Luminescence dating of Würmian (Weichselian) proglacial sediments from Switzerland: methodological aspects and stratigraphical conclusions. *Boreas* **36**, 130–142.
- Preusser, F., Büschelberger, M., Kemna, H.A., Miocic, J., Mueller, D., May, J.-H., 2021. Exploring possible links between Quaternary aggradation in the Upper Rhine Graben and the glaciation history of northern Switzerland. *International Journal of Earth Sciences* **110**, 1827–1846. <https://doi.org/10.1007/s00531-021-02043-7>
- Preusser, F., Drescher-Schneider, R., Fiebig, M., Schlüchter, C., 2005. Re-interpretation of the Meikirch pollen record, Swiss Alpine Foreland, and implications for Middle Pleistocene chronostratigraphy. *Journal of Quaternary Science* **20**, 607–620.
- Preusser, F., Geyh, M.A., Schlüchter, C., 2003. Timing of Late Pleistocene climate change in lowland Switzerland. *Quaternary Science Reviews* **22**, 1435–1445.
- Preusser, F., Graf, H., 2002. Erste ergebnisse von lumineszenzdatierungen eiszeitlicher ablagerungen der Nordschweiz. *Jahresberichte und Mitteilungen des Oberrheinischen Geologischen Vereins* **84**, 419–438.
- Preusser, F., Graf, H.R., Keller, O., Krayss, E., Schlüchter, C., 2011. Quaternary glaciation history of Northern Switzerland. *E&G Quaternary Science Journal* **60**, 282–305.
- Preusser, F., Schlüchter, C., 2004. Dates from an important early Late Pleistocene ice advance in the Aare valley, Switzerland. *Eclogae Geologicae Helveticae* **97**, 245–253.
- Reber, R., Akçar, N., Ivy-Ochs, S., Tikhomirov, D., Burkhalter, R., Zahno, C., Lüthold, A., Kubik, P.W., Vockenhuber, C., Schlüchter, C., 2014. Timing of retreat of the Reuss Glacier (Switzerland) at the end of the last glacial maximum. *Swiss Journal of Geosciences* **107**, 293–307. <https://doi.org/10.1007/s00015-014-0169-5>
- Schaller, S., Buechi, M.W., Schuster, B., Anselmetti, F.S., 2023. Drilling into a deep buried valley (ICDP DOVE): a 252 m long sediment succession from a glacial overdeepening in northwestern Switzerland. *Scientific Drilling* **32**, 27–42.
- Schlüchter, C., 1975. Schotterpetrologie und deren relativ-stratigraphische anwendbarkeit im Aaretal südlich von Bern (Schweiz). *Eiszeitalter und Gegenwart* **26**, 74–81.
- Schlüchter, C., 1989. Thalgut—a comprehensive Quaternary record of the northern Swiss alpine foreland. *Eclogae Geologicae Helveticae* **82**, 277–284.
- Schlüchter, C., 1997. Sedimente des Gletschers (Teil I). *Bulletin für Angewandte Geologie* **2**, 99–112.
- Schlüchter, C., Akçar, N., Ivy-Ochs, S., 2021. The Quaternary Period in Switzerland. In: Reynard, E. (Ed.), *Landscapes and Landforms of Switzerland. World Geomorphological Landscapes*. Springer, Cham, pp. 47–69. https://doi.org/10.1007/978-3-030-43203-4_4
- Schlunegger, F., Matter, A., Mange, M.A., 1993. Alluvial fan sedimentation and structure of the southern Molasse Basin margin, Lake Thun area, Switzerland. *Eclogae Geologicae Helveticae* **86**, 717–750.
- Schlunegger, F., Mosar, J., 2011. The last erosional stage of the Molasse Basin and the Alps. *International Journal of Earth Sciences* **100**, 1147–1162.
- Schultheiss, P.J., Weaver, P.P.E., 1992. Multi-sensor core logging for science and industry. In: *OCEANS'92. Mastering the Oceans Through Technology*. Newport, RI, pp. 608–613. <https://doi.org/10.1109/OCEANS.1992.607652>
- Schuster, B., Gegg, L., Schaller, S., Buechi, M.W., Tanner, D.C., Wielandt-Schuster, U., Anselmetti, F.S., Preusser, F., 2024. Shaped and filled by the

- Rhine Glacier: the overdeepened Tannwald Basin in southwestern Germany. *Scientific Drilling* **33**, 191–206.
- Schwenk, M.A., Schläfli, P., Bandou, D., Gribenski, N., Douillet, G.A., Schlunegger, F., 2022a. From glacial erosion to basin overfill: a 240 m-thick overdeepening–fill sequence in Bern, Switzerland. *Scientific Drilling* **30**, 17–42.
- Schwenk, M.A., Stutenbecker, L., Schläfli, P., Bandou, D., Schlunegger, F., 2022b. Two glaciers and one sedimentary sink: the competing role of the Aare and the Valais glaciers in filling an overdeepened trough inferred from provenance analysis. *E&G Quaternary Science Journal* **71**, 163–190.
- Seguinot, J., Ivy-Ochs, S., Juvet, G., Huss, M., Funk, M., Preusser, F., 2018. Modelling last glacial cycle ice dynamics in the Alps. *The Cryosphere* **12**, 3265–3285.
- Seidel, M., Hlawitschka, M., 2015. An R-based function for modeling of end member compositions. *Mathematical Geosciences* **47**, 995–1007.
- Serra, O., Sulpice, L., 1975. Sedimentological analysis of shale–sand series from well logs. SPWLA 16th Annual Logging Symposium, New Orleans, Louisiana, June 1975. Society of Petrophysicists and Well-Log Analysts, SPWLA-1975-W.
- Smedley, R.K., Chiverrell, R.C., Ballantyne, C.K., Burke, M.J., Clark, C.D., Duller, G.A.T., Fabel, D., McCarroll, D., Scourse, J.D., Small, D., 2017. Internal dynamics condition centennial-scale oscillations in marine-based ice-stream retreat. *Geology* **45**, 787–790.
- Swisstopo, 2011. *SwissALTI3D*. Federal Office of Topography Swisstopo, Wabern, Switzerland.
- Thew, N., Kälin, D., Cuenca-Bescós, G., Buechi, M. W., Penkman, K., Scheidt, S., Knipping, M., Maier, F., Urresti, I., Deplazes, G., 2024. The Hasli Formation of the Irchel Plateau—a key record for older Early Pleistocene interglacial sediments in Northern Switzerland. *Quaternary Science Reviews* **332**, 108550. <https://doi.org/10.1016/j.quascirev.2024.108550>
- Tomonaga, Y., Buechi, M.W., Deplazes, G., Kipfer, R., 2024. First dating of an early Chibanian (Middle Pleistocene) glacial overdeepening in the Alpine Foreland using the $^4\text{He}/\text{U}$ –Th method. *Geology* **53**, 40–44. <https://doi.org/10.1130/G52544.1>
- van Zyl, J.J., 2001. The Shuttle Radar Topography Mission (SRTM): a breakthrough in remote sensing of topography. *Acta Astronautica* **48**, 559–565.
- Wyssling, L., Wyssling, G., 1978. Interglaziale see-ablagerungen in einer bohrung bei Uster (Kanton Zürich). *Eclogae Geologicae Helvetiae* **71**, 357–375.
- Yanites, B.J., Becker, J.K., Madritsch, H., Schnellmann, M., Ehlers, T.A., 2017. Lithologic effects on landscape response to base level changes: a modeling study in the context of the Eastern Jura Mountains, Switzerland. *Journal of Geophysical Research: Earth Surface* **122**, 2196–2222.
- Ziegler, P.A., Fraefel, M., 2009. Response of drainage systems to Neogene evolution of the Jura fold-thrust belt and Upper Rhine Graben. *Swiss Journal of Geosciences* **102**, 57–75.
- Zolitschka, B., Francus, P., Ojala, A.E.K., Schimmelmann, A., 2015. Varves in lake sediments—a review. *Quaternary Science Reviews* **117**, 1–41.